effect of the transient expressions of apoE4(1–272) and apoE4(1–299) on ATP synthesis and membrane potential in Neuro2a cells. Unexpectedly, there was no difference between apoE4(1–272)- and apoE4(1–299)-transfected cells in terms of the levels of ATP synthesis or membrane potential (Fig. 6). However, when we tried to generate the Neuro2a cells, in which apoE4(1–272) is stably expressed, all the cells were dead within 2 weeks after the transfection, whereas apoE4(1–299)-expressing cells remained alive. These results suggest that apoE4(1–272) may have neurotoxicity as previously reported [29], although the level of toxicity is low. This issue remains to be addressed in further studies.

One may consider that apoE is synthesized as a secretory protein; however, how apoE enters the cytosol remains unclear and controversial. Previous studies have shown that apoE escapes the secretory or endosomal internalization pathway, and enters the cytosol of neuronal cells [25,29,40] and non-neuronal cells [41], whereas another study has failed to show this [42]. Therefore, the physiological relevance of the three mitochondrial proteins that we have identified in this study, which are associated with apoE, remains to be confirmed under physiological conditions.

It is well known that apoE4 is a strong risk factor for AD development, and the regulation of apoE4 function may be a therapeutic target for AD. Our findings indicate that if we could modulate the generation of apoE4(1–272) and/or modulate its translocation to mitochondria, the apoE4-associated induction of neurodegeneration could be prevented or attenuated. Because it has been shown that the C-terminus of the apoE-cleaving enzyme is a neuron-specific, chymotrypsin-like serine protease [25-27], the characterization and modulation of this enzyme activity would be a therapeutic target for AD.

## Conclusion
We identified intracellular apoE-binding molecules and determined their functions in modulating mitochondria function. The ApoE-binding molecules we found are ubiquinol cytochrome *c* reductase core protein 2 (UQCRC2), cytochrome C1, and cytochrome *c* oxidase subunit 4 isoform 1 (COX IV 1). The UQCRC2 and cytochrome C1 are components of mitochondrial respiratory complex III, and COX IV 1 is a component of complex IV. Interestingly, these proteins associated with apoE4(1–272) more strongly than intact apoE4 (1–299). When apoE4(1–272) expression level increased in Neuro2a cells, the enzymatic activities of mitochondrial respiratory complexes III and IV were significantly lower than those in Neuro-2a cells expressing apoE4(1–299). These results suggest that the

C-terminal-truncated fragment of apoE4(1–272) bind to mitochondrial complexes and affects their activities.

## Methods
### Preparation of mouse brain membrane extracts and cytosolic fraction
Brains obtained from C57BL6 male mice were homogenized with a homogenizing buffer (10 mM Tris-HCl, pH 7.4 1 mM EDTA 0.25 M sucrose), and the homogenate was centrifuged at 1,000 *g* for 10 min at 4°C. The supernatant was recentrifuged at 10,000 *g* for 20 min at 4°C, and the resulting precipitate was suspended in a homogenizing buffer. The supernatant was recentrifuged at 100,000 *g* for 1 min at 4°C, and the resulting precipitate was suspended in a homogenizing buffer. The supernatant was used as the cytosolic fraction. The proteins in the 10,000 *g* and 100,000 *g* pellet fraction were extracted with homogenizing buffer containing 1 M KCl. The resulting pellet was solubilized with 2% Triton X-100 for 1 h at 4°C and then centrifuged at 100,000 *g* of 1 h at 4°C. The supernatants were used as 10,000 *g* or 100,000 *g* membrane extracts.

### FLAG fusion proteins
Recombinant FLAG-apoE4 fusion proteins encoding WT (1–299) or C-terminal truncated apoE4 (1–272) were prepared and purified as follows. PCR products encoding apoE4 (1–272) and apoE4 (1–299) were subcloned into pFLAG-MAC expression vector (Sigma). These plasmids were transformed into the BL21 strain of *Escherichia coli* and induced with isopropyl-1-thio-b-$_D$-galactopyranoside to produce FLAG fusion proteins. The bacteria were suspended in PBS, and vigorous sonication was performed before centrifugation at 10,000 *g* for 20 min. The resulting supernatants were applied to anti-FLAG M2-agarose affinity resin column (Sigma) and then eluted with an elution buffer (TBS containing 100 μg/ml FLAG peptide (Sigma)). Purified FLAG fusion proteins were dialyzed against TBS.

### FLAG-ApoE4 affinity chromatography and LC-MS/MS analysis
Recombinant FLAG-apoE4(1–299) or FLAG-apoE4(1–272) fusion protein coupled to anti-FLAG M2-agarose affinity resin was used to identify affinity-purified apoE4-binding proteins. The fractionated mouse brain samples were applied to the FLAG-apoE4(1–299)- and FLAG-apoE4(1–272)-anti-FLAG M2-agarose affinity resin column. The proteins bound to the resin column were then eluted with the elution buffer. The eluted proteins were dialyzed against the dialysis buffer, concentrated, and subjected to SDS-PAGE. The gels were stained with Silver-Quest Silver Staining kit (Invitrogen). The proteins specifically associated with apoEs demonstrated as silver-

stained bands were cut out, digested with trypsin, and subjected to LC-MS/MS analysis.

### LC-MS/MS analysis

The proteins in the silver-stained bands were reduced with 10 mM dithiothreitol at room temperature for 2 h and alkylated with 40 mM iodoacetamide in the dark at room temperature for 30 min. Each sample was digested with trypsin (4 µg/ml; Trypsin Gold, Promega) in 40 mM $NH_4HCO_3$/10%ACN at 37°C overnight. The extracted peptides were then separated via nano liquid chromatography (LC) (Paradigm MS4, Michrom BioResources, Inc., Auburn, CA) using a Magic C18 column (0.2 × 50 mm; Michrom BioResources, Inc.; Auburn, CA). The LC eluent was analyzed using an LCQ Advantage MAX mass spectrometer (Thermo Fisher Scientific) equipped with an ionspray source. All MS/MS spectra were searched by SEQUEST algorithm from BioWorks software (Thermo Fisher Scientific).

### Cells

Neuro2a cells were grown in DMEM medium, supplemented with 10% FBS, 50 units/ml penicillin, 50 mg/ml streptomycin, and 2 mM glutamine at 37°C in a humidified 5% $CO_2$ 95% air incubator.

### Transfection of plasmids into cells and co-immunopricipitation

PCR products encoding apoE4 (1–272) and apoE4 (1–299) were subcloned into pFLAG-CMV-2 expression vector (Sigma). Neuro2a cells were co-transfected with FLAG-apoE4 (1–272 or 1–299) plasmids and mammalian expression plasmids coding the candidate of apoE4 associating proteins (Toyobo, Japan) using Lipofectamine 2000 (Invitrogen, CA, USA). As necessary, mammalian expression plasmids coding the candidate apoE4-associated proteins were fused with HA-tag of their C-terminus using KOD-PLUS Mutagenesis Kit (Toyobo). The plasmids were transfected to Neuro2a cells as follows. Neuro2a cells were plated on a 6-cm plate at a cell density of 1.5 × 10⁶ and cultured in the culture medium described above. The next day, the ells were transfected with the plasmid employing Lipofectamine 2000 reagent. On culture day 3, the cells were lysed with 500 µl of Triton X-100 solubilization buffer (10 mM Tris-HCl (pH 7.4), 150 mM NaCl, 1 mM EDTA, 10 mg/ml leupeptin, 1 mM PMSF, 0.5% Triton X-100). The cell lysate was incubated with anti-FLAG M2-agarose affinity resin. After an overnight incubation at 4°C, the beads were washed three times with Triton X-100 solubilization buffer and then eluted with the elution buffer (PBS containing FLAG peptide at a concentration of 100 µg/ml). The immunoprecipitates were then analyzed by western blotting with anti-HA monoclonal antibody (Sigma), anti-UQCRC2 monoclonal antibody (Abcam), and anti-COX IV 1 monoclonal antibody (Cell Signaling).

### Enzymatic analysis of complexes III and IV

Mitochondria isolated from homogenates of Neuro2a cells transfected with ApoE4 (1–299 or 1–272) were used for enzymatic analysis.

#### (a) Complex III (Ubiquinol cytochrome c reductase)

The oxidation of ubiquinol₂ by complex III was determined using cytochrome c (III) as an electron acceptor. The assay was carried out in an assay medium (25 mM potassium phosphate buffer (pH 8.0), 1 mM EDTA, 1 mM KCN, 3 mM $Na_3N$) supplemented with 20 µM cytochrome c (III), and 20 µM ubiquinol₂. The reaction was started with 5 µg of mitochondrial protein and the enzyme activity was measured at 550 nm. The activity of complex III is estimated to be the difference in the reduction of cytochrome c with and without 10 µg/ml antimycin A and 10 µg/ml myxothiazol.

#### (b) Complex IV (Cytochrome c Oxidase)

The enzyme activity of cytochrome c oxidase (complex IV) was determined using Mitochondria Activity Assay kit (BioChain Institute, U.S.A.) and performed following the manufacture's procedure. Complex IV activity was measured as the oxidation of ferrocytochrome c by cytochrome c oxidase at 550 nm. Complex IV activity is expressed as the difference in the oxidation of ferrocytochrome C with or without KCN and $Na_3N$ as complex IV inhibitor.

### ATP synthase activity assay

Neuro2a cells transfected with apoE4(1–272) and apoE4(1–299) plasmids were harvested and homogenized with a homogenizing buffer (10 mM Tris-HCl, pH 7.4, 1 mM EDTA, 0.25 M sucrose), and the homogenate was centrifuged at 1,000 g for 10 min at 4°C. The resulting supernatant was further centrifuged at 10,000 × g for 20 min at 4°C, and the resulting pellet (ppt) fractions were obtained. The ppt fractions were resuspended in 100 µl of assay buffer (1 mM ADP and 5 mM sodium succinate) and incubated for 5 min at 37°C. 100 mM Tris-HCl buffer (pH 7.6) containing 4 mM EDTA was added and the fractions were further incubated for 2 min at 100°C. Then the fractions were plated on ice and ATP level in each fraction was determined using an ATP bioluminescence assay kit CLS II (Roche Diagnosis GmbH, Mannheim, Germany).

### Analysis of mitochondrial membrane potential (mt )

ApoE4(1–272) or 1–299)-transfected Neuro2a cells were stained with 2 µM JC-1 (Molecular Probes, Eugene, OR) at 37°C for 20 min. Then, the cells were analyzed using a flow cytometer FACSCalibur (Becton Dickinson, Franklin Lakes, NJ) with FlowJo software (Tree Star Inc., Ashland, OR).

### Statistical analysis

StatView computer software (Windows) was used for statistical analysis. Statistical significance of differences

between samples was evaluated by multiple pairwise comparisons among the sets of data using ANOVA and the Bonferoni t-test.

## Competing interests

The authors declare that they have no competing interests.

## Authors' contributions

TN carried out major part of the experiments. AW carried out TOF-MS/MS analysis and identified molecules associated with apoE. TF generated plasmid containing intact apoE3 and apoE4 cDNA. TH prepared cultured cells. MM designed this study and was involved in the interpretation of the results and in drafting the manuscript.

## Acknowledgements

## References

1.  Strittmatter WJ, Saunders AM, Schmechel D, Pericak-Vance M, Enghild J, Salvesen GS, Roses AD: **Apolipoprotein E: high-avidity binding to beta-amyloid and increased frequency of type 4 allele in late-onset familial Alzheimer disease.** *Proc Natl Acad Sci USA* 1993, **90:**1977-1981.

2.  Roses AD: **Apolipoprotein E affects the rate of Alzheimer disease expression: beta-amyloid burden is a secondary consequence dependent on APOE genotype and duration of disease.** *J Neuropathol Exp Neurol* 1994, **53:**429-37.

3.  Corder EH, Saunders AM, Strittmatter WJ, Schmechel DE, Gaskell PC, Small GW, Roses AD, Haines JL, Pericak-Vance MA: **Gene dose of apolipoprotein E type 4 allele and the risk of Alzheimer's disease in late onset families.** *Science* 1993, **261:**921-923.

4.  Wollmer MA, Streffer JR, Lutjohann D, Tsolaki M, Iakovidou V, Hegi T, Pasch T, Jung HH, Bergmann K, Nitsch RM, Hock C, Papassotiropoulos A: **ABCA1 modulates CSF cholesterol levels and influences the age at onset of Alzheimer's disease.** *Neurobiol Aging* 2003, **24:**421-426.

5.  Kolsch H, Lutjohann D, Ludwig M, Schulte A, Ptok U, Jessen F, von Bergmann K, Rao ML, Maier W, Heun R: **Polymorphism in the cholesterol 24S-hydroxylase gene is associated with Alzheimer's disease.** *Mol Psychiatry* 2002, **7:**899-902.

6.  Papassotiropoulos A, Streffer JR, Tsolaki M, Schmid S, Thal D, Nicosia F, Iakovidou V, Maddalena A, Lutjohann D, Ghebremedhin E, Hegi T, Pasch T, Traxler M, Bruhl A, Benussi L, Binetti G, Braak H, Nitsch RM, Hock C: **Increased brain beta-amyloid load, phosphorylated tau, and risk of Alzheimer disease associated with an intronic CYP46 polymorphism.** *Arch Neurol* 2003, **60:**29-35.

7.  Mahley RW: **Apolipoprotein E: cholesterol transport protein with expanding role in cell biology.** *Science* 1988, **240:**622-630.

8.  Mahley RW, Huang Y: **Apolipoprotein E: from atherosclerosis to Alzheimer's disease and beyond.** *Curr Opin Lipidol* 1999, **10:**207-17.

9.  Mahley RW, Rall SC Jr: **Apolipoprotein E: far more than a lipid transport protein.** *Annu Rev Genomics Hum Genet* 2000, **1:**507-37.

10. Farrer LA, Cupples LA, Haines JL, Hyman B, Kukull WA, Mayeux R, Myers RH, Pericak-Vance MA, Risch N, van Duijn CM: **Effects of age, sex, and ethnicity on the association between apolipoprotein E genotype and Alzheimer disease. A meta-analysis. APOE and Alzheimer Disease Meta Analysis Consortium.** *JAMA* 1997, **278:**1349-1356.

11. Roheim PS, Carey M, Forte T, Vega GL: **Apolipoproteins in human cerebrospinal fluid.** *Proc Natl Acad Sci USA* 1979, **76:**4646-4649.

12. Pitas RE, Boyles JK, Lee SH, Hui D, Weisgraber KH: **Lipoproteins and their receptors in the central nervous system. Characterization of the lipoproteins in cerebrospinal fluid and identification of apolipoprotein B, E(LDL) receptors in the brain.** *J Biol Chem* 1987, **262:**14352-14360.

13. Krimbou L, Denis M, Haidar B, Carrier M, Marcil M, Genest J: **Molecular interactions between apolipoprotein E and the ATP-binding cassette transporter A1 (ABCA1): Impact on ApoE lipidation.** *J Lipid Res* 2004, **45:**839-848.

14. Ito J, Zhang LY, Asai M, Yokoyama S: **Differential generation of high-density lipoprotein by endogenous and exogenous apolipoproteins in cultured fetal rat astrocytes.** *J Neurochem* 1999, **72:**2362-2369.

15. Michikawa M, Fan QW, Isobe I, Yanagisawa K: **Apolipoprotein E exhibits isoform-specific promotion of lipid efflux from astrocytes and neurons in culture.** *J Neurochem* 2000, **74:**1008-1016.

16. Gong JS, Kobayashi M, Hayashi H, Zou K, Sawamura N, Fujita SC, Yanagisawa K, Michikawa M: **Apolipoprotein E (ApoE) isoform-dependent lipid release from astrocytes prepared from human ApoE3 and ApoE4 knock-in mice.** *J Biol Chem* 2002, **277:**29919-29926.

17. Xu Q, Brecht WJ, Weisgraber KH, Mahley RW, Huang Y: **Apolipoprotein E4 domain interaction occurs in living neuronal cells as determined by fluorescence resonance energy transfer.** *J Biol Chem* 2004, **24:**25511-25516.

18. Gong JS, Morita SY, Kobayashi M, Handa T, Fujita SC, Yanagisawa K, Michikawa M: **Novel action of apolipoprotein E (ApoE): ApoE isoform specifically inhibits lipid-particle-mediated cholesterol release from neurons.** *Mol Neurodegener* 2007, **2:**9.

19. Mauch DH, Nagler K, Schumacher S, Goritz C, Muller EC, Otto A, Pfrieger FW: **CNS synaptogenesis promoted by glia-derived cholesterol.** *Science* 2001, **294:**1354-7.

20. Hayashi H, Campenot RB, Vance DE, Vance JE: **Glial lipoproteins stimulate axon growth of central nervous system neurons in compartmented cultures.** *J Biol Chem* 2004, **279:**14009-15.

21. Heeren J, Grewal T, Laatsch A, Becker N, Rinninger F, Rye K-A, Beisiegel U: **Impaired Recycling of Apolipoprotein E4 Is Associated with Intracellular Cholesterol Accumulation.** *J Biol Chem* 2004, **279:**55483-55492.

22. Fassbender K, Simons M, Bergmann C, Stroick M, Lutjohann D, Keller P, Runz H, Kuhl S, Bertsch T, von Bergmann K, Hennerici M, Beyreuther K, Hartmann T: **Simvastatin strongly reduces levels of Alzheimer's disease beta-amyloid peptides Abeta 42 and Abeta 40 in vitro and in vivo.** *Proc Natl Acad Sci USA* 2001, **98:**5856-61.

23. Cole SL, Vassar R: **The Alzheimer's disease beta-secretase enzyme, BACE1.** *Mol Neurodegener* 2007, **2:**22.

24. Cam JA, Zerbinatti CV, Li Y, Bu G: **Rapid endocytosis of the low density lipoprotein receptor-related protein modulates cell surface distribution and processing of the beta-amyloid precursor protein.** *J Biol Chem* 2005, **280:**15464-70.

25. Huang Y, Liu XQ, Wyss-Coray T, Brecht WJ, Sanan DA, Mahley RW: **Apolipoprotein E fragments present in Alzheimer's disease brains induce neurofibrillary tangle-like intracellular inclusions in neurons.** *Proc Natl Acad Sci USA* 2001, **98:**8838-43.

26. Brecht WJ, Harris FM, Chang S, Tesseur I, Yu GQ, Xu Q, Dee Fish J, Wyss-Coray T, Buttini M, Mucke L, Mahley RW, Huang Y: **Neuron-specific apolipoprotein e4 proteolysis is associated with increased tau phosphorylation in brains of transgenic mice.** *J Neurosci* 2004, **24:**2527-34.

27. Harris FM, Brecht WJ, Xu Q, Tesseur I, Kekonius L, Wyss-Coray T, Fish JD, Masliah E, Hopkins PC, Scearce-Levie K, Weisgraber KH, Mucke L, Mahley RW, Huang Y: **Carboxyl-terminal-truncated apolipoprotein E4 causes Alzheimer's disease-like neurodegeneration and behavioral deficits in transgenic mice.** *Proc Natl Acad Sci USA* 2003, **100:**10966-71.

28. Fan D, Li Q, Korando L, Jerome WG, Wang J: **A monomeric human apolipoprotein E carboxyl-terminal domain.** *Biochemistry* 2004, **43:**5055-64.

29. Chang S, Ma Tr, Miranda RD, Balestra ME, Mahley RW, Huang Y: **Lipid- and receptor-binding regions of apolipoprotein E4**

fragments act in concert to cause mitochondrial dysfunction and neurotoxicity. *Proceedings of the National Academy of Sciences* 2005, 102:18694-18699.

30. Mahley RW, Hui DY, Innerarity TL, Beisiegel U: Chylomicron remnant metabolism. Role of hepatic lipoprotein receptors in mediating uptake. *Arteriosclerosis* 1989, 9:114-8.
31. Tanaka M, Vedhachalam C, Sakamoto T, Dhanasekaran P, Phillips MC, Lund-Katz S, Saito H: Effect of carboxyl-terminal truncation on structure and lipid interaction of human apolipoprotein E4. *Biochemistry* 2006, 45:4240-7.
32. Pillot T, Goethals M, Najib J, Labeur C, Lins L, Chambaz J, Brasseur R, Vandekerckhove J, Rosseneu M: Beta-amyloid peptide interacts specifically with the carboxy-terminal domain of human apolipoprotein E: relevance to Alzheimer's disease. *J Neurochem* 1999, 72:230-7.
33. Phu MJ, Hawbecker SK, Narayanaswami V: Fluorescence resonance energy transfer analysis of apolipoprotein E C-terminal domain and amyloid beta peptide (1–42) interaction. *J Neurosci Res* 2005, 80:877-86.
34. Caspersen C, Wang N, Yao J, Sosunov A, Chen X, Lustbader JW, Xu HW, Stern D, McKhann G, Yan SD: Mitochondrial Abeta: a potential focal point for neuronal metabolic dysfunction in Alzheimer's disease. *Faseb J* 2005, 19:2040-1.
35. Takahashi RH, Milner TA, Li F, Nam EE, Edgar MA, Yamaguchi H, Beal MF, Xu H, Greengard P, Gouras GK: Intraneuronal Alzheimer abeta42 accumulates in multivesicular bodies and is associated with synaptic pathology. *Am J Pathol* 2002, 161:1869-79.
36. Martin BL, Schrader-Fischer G, Busciglio J, Duke M, Paganetti P, Yankner BA: Intracellular Accumulation of beta-Amyloid in Cells Expressing the Swedish Mutant Amyloid Precursor Protein. *J Biol Chem* 1995, 270:26727-26730.
37. Chui DH, Tanahashi H, Ozawa K, Ikeda S, Checler F, Ueda O, Suzuki H, Araki W, Inoue H, Shirotani K, Takahashi K, Gallyas F, Tabira T: Transgenic mice with Alzheimer presenilin 1 mutations show accelerated neurodegeneration without amyloid plaque formation. *Nat Med* 1999, 5:560-4.
38. Wilson CA, Doms RW, Lee VM: Intracellular APP processing and A beta production in Alzheimer disease. *J Neuropathol Exp Neurol* 1999, 58:787-94.
39. Hartmann T: Intracellular biology of Alzheimer's disease amyloid beta peptide. *Eur Arch Psychiatry Clin Neurosci* 1999, 249:291-8.
40. Lovestone S, Anderton BH, Hartley C, Jensen TG, Jorgensen AL: The intracellular fate of apolipoprotein E is tau dependent and apoe allele-specific. *Neuroreport* 1996, 7:1005-8.
41. Hamilton RL, Wong JS, Guo LS, Krisans S, Havel RJ: Apolipoprotein E localization in rat hepatocytes by immunogold labeling of cryothin sections. *J Lipid Res* 1990, 31:1589-603.
42. DeMattos RB, Thorngate FE, Williams DL: A test of the cytosolic apolipoprotein E hypothesis fails to detect the escape of apolipoprotein E from the endocytic pathway into the cytosol and shows that direct expression of apolipoprotein E in the cytosol is cytotoxic. *J Neurosci* 1999, 19:2464-73.

Neurobiology

# Microglia Activated with the Toll-Like Receptor 9 Ligand CpG Attenuate Oligomeric Amyloid β Neurotoxicity in in Vitro and in Vivo Models of Alzheimer's Disease

Yukiko Doi,* Tetsuya Mizuno,* Yuki Maki,*
Shijie Jin,* Hiroyuki Mizoguchi,[†]
Masayoshi Ikeyama,[‡] Minoru Doi,[‡]
Makoto Michikawa,[§] Hideyuki Takeuchi,*
and Akio Suzumura*

From the Department of Neuroimmunology* and the Futuristic
Environmental Simulation Center,[†] Research Institute of
Environmental Medicine, Nagoya University, Nagoya; the
Department of Materials Science and Engineering,[‡] Nagoya
Institute of Technology, Nagoya; and the Department of
Alzheimer's Disease Research,[§] National Institute for Longevity
Sciences, National Center for Geriatrics and Gerontology,
Aichi, Japan

**Soluble oligomeric amyloid β (oAβ) 1-42 causes synaptic dysfunction and neuronal injury in Alzheimer's disease (AD). Although accumulation of microglia around senile plaques is a hallmark of AD pathology, the role of microglia in oAβ1-42 neurotoxicity is not fully understood. Here, we showed that oAβ but not fibrillar Aβ was neurotoxic, and microglia activated with unmethylated DNA CpG motif (CpG), a ligand for Toll-like receptor 9, attenuated oAβ1-42 neurotoxicity in primary neuron-microglia co-cultures. CpG enhanced microglial clearance of oAβ1-42 and induced higher levels of the antioxidant enzyme heme oxygenase-1 in microglia without producing neurotoxic molecules such as nitric oxide and glutamate. Among subclasses of CpGs, class B and class C activated microglia to promote neuroprotection. Moreover, intracerebroventricular administration of CpG ameliorated both the cognitive impairments induced by oAβ1-42 and the impairment of associative learning in Tg2576 mouse model of AD. We propose that CpG may be an effective therapeutic strategy for limiting oAβ1-42 neurotoxicity in AD. (Am J Pathol 2009, 175:2121–2132; DOI: 10.2353/ajpath.2009.090418)**

The senile plaque is a pathological hallmark of Alzheimer's disease (AD). Fibrillar amyloid β (fAβ), a major component of senile plaques, induces tau hyperphosphorylation and neuronal dystrophy.[1,2] Soluble oligomeric Aβ (oAβ) has been reported to exhibit higher neurotoxicity than fAβ. Naturally secreted oAβ inhibits hippocampal long-term potentiation and disrupts synaptic plasticity in rats in vivo[3]. In addition, oAβ induces neuronal reactive oxygen species (ROS) through a mechanism requiring N-methyl-D-aspartate receptor activation.[4] Exposure to oAβ induces rapid and massive neuronal death, while fAβ is required at higher concentrations and for longer incubations to cause neuronal dystrophy.[5]

Microglia, macrophage-like cells in the central nervous system, cluster both in and around senile plaques and have been proposed to have pivotal roles in the pathogenesis of AD. Microglia activated with Aβ may be involved in the inflammatory component of AD.[6] Both fAβ and oAβ stimulate microglial secretion of proinflammatory cytokines, chemokines, complement components, and free radicals.[7] However, microglia also perform neu-

roprotective functions such as releasing neurotrophic factors[8] and phagocytosing and degrading Aβ.[9,10]

Toll-like receptor (TLR) ligands enhance microglial phagocytosis of Aβ. Peptidoglycan, a TLR2 ligand, and unmethylated DNA CpG motifs (CpG), a TLR9 ligand, increase Aβ phagocytosis through the G protein-coupled formyl peptide receptor-like 2.[11,12] Similarly, the TLR4 ligand lipopolysaccharide increases phagocytosis through the CD14 receptor.[13] However, microglia activated with TLR ligands also produce neurotoxic molecules such as proinflammatory cytokines, nitric oxide (NO), ROS, and peroxynitrite.[14] In particular, lipopolysaccharide-activated microglia produce a large amount of glutamate, a neurotransmitter but also potent neurotoxin.[15] Thus, factors that increase microglial clearance of oAβ without producing inflammatory mediators are candidates for the treatment of AD.

Here, we investigated the role of microglia in neurotoxicity mediated by oAβ1-42. We found that microglia activated with a low dose of CpG attenuated the neurotoxic effects of oAβ1-42 without producing other neurotoxic molecules *in vitro*. Moreover, intracerebroventricular (ICV) administration of CpG ameliorated the cognitive impairment induced by ICV injection of oAβ1-42 and the impairment of associative learning in Tg2576 mouse model of AD.

## Materials and Methods

### Cell Culture

The protocols for animal experiments were approved by the Animal Experiment Committee of Nagoya University. Primary neuronal cultures were prepared from the cortices of embryonic day 17 (E17) C57BL/6 mice embryos as described previously.[8] Briefly, cortical fragments were dissociated into single cells in dissociation solution (Sumitomo Bakelite, Akita, Japan) and resuspended in Nerve Culture Medium (Sumitomo Bakelite). Neurons were plated onto 12-mm-polyethyleneimine-coated glass coverslips (Asahi Techno Glass, Chiba, Japan) at a density of 5 × 10⁴ cells/well in 24-well multidishes and incubated at 37°C in a humidified atmosphere containing 5% $CO_2$. The purity of the cultures was >95% as determined by NeuN-specific immunostaining. Microglia were isolated on 14 days *in vitro* with the "shaking off" method previously described from primary mixed glial cell cultures prepared from newborn C57BL/6 mice.[16] Cultures were 97 to 100% pure as determined by Fc receptor-specific immunostaining and were maintained in Dulbecco's modified Eagle medium supplemented with 10% fetal calf serum, 5 μg/ml bovine insulin, and 0.2% glucose. Microglia were plated at a density of 7 × 10⁴ cells/well in 8-well glass slides or at a density of 7 × 10⁴ cells/well in 48-well multidishes. Neuron-microglia co-cultures were prepared as follows: 1 × 10⁵ microglia in 100 μl of neuronal medium were added to neuronal cultures (5 × 10⁴ neuronal cells) on 13 day *in vitro* in 24-well multidishes.

### Preparations of Aβ Solutions

fAβ1-42 was prepared as described previously.[17] Briefly, synthetic human Aβ1-42 (Peptide Institute, Osaka, Japan) was dissolved in 0.02% ammonia solution at a concentration of 250 μmol/L, diluted to 25 μmol/L in PBS, and incubated at 37°C for 24 hours. oAβ1-42 was prepared as described previously.[18] Briefly, Aβ1-42 was dissolved to 1 mmol/L in 100% 1,1,1,3,3,3-hexafluoro-2-propanol. 1,1,1,3,3,3-Hexafluoro-2-propanol was dried by the vacuum desiccator and resuspended to 5 mmol/L in DMSO. To form oligomers, amyloid peptide was diluted to a final concentration of 100 μmol/L with Ham's F-12 and incubated at 4°C for 24 hours and then immediately added to cultures at a final concentration 5 μmol/L.

### Transmission Electron Microscopy

To assess quaternary structures of Aβ, oAβ1-42 and fAβ1-42 solutions were spread on carbon-coated grids. Negative staining was performed with 3% phosphotungstic acid (pH 7.0). Proteins were then examined with a JEM-2000ExII Electron Microscope with an acceleration voltage of 160 kV.

### Thioflavin T Assay

Optimum fluorescence measurements of amyloid fibrils were obtained at excitation and emission wavelength of 446 and 490 nm, respectively, with a reaction mixture containing 5 μmol/L thioflavin T (Nakalai tesque, Kyoto, Japan) and 50 mmol/L glycine-NaOH buffer (pH 8.5). Ten microliters of oAβ1-42 or fAβ1-42 solution was mixed with 100 μl of the reaction mixture, respectively.

### Measurement of Heme Oxygenase-1, Interleukin-10, Matrix Metalloproteinase-9, Tumor Necrosis Factor-α, NO, and Glutamate

To measure factors produced by microglia treated with CpG and oAβ1-42, microglia were plated at a density of 7 × 10⁴ cells/well (300 μl) in 48-well multidishes and then treated with 100 nmol/L CpG-DNA (HyCult Biotechnology, Uden, Netherlands), 100 nmol/L class A CpG (synthetic oligodeoxynucleotides (ODNs) 1585), class B CpG (ODN 1668), and class C CpG (ODN 2395). These CpG subtypes were from Alexis Biochemicals (San Diego, CA). After 3 hours of treatment with CpG, 5 μmol/L oAβ1-42 was added for 24 hours. Supernatants from microglia were assessed by ELISA kits for tumor necrosis factor-α (TNF-α) and interleukin (IL)-10 (BD Pharmingen, Franklin Lakes, NJ) and matrix metalloproteinase (MMP)-9 (R&D Systems, Minneapolis, MN). Cell extracts from microglia in extraction buffer (1% Nonidet P-40 in PBS) were measured for heme oxygenase-1 (HO-1) with an ELISA kit (Takara Bio, Mie, Japan). Measurement of NO was determined using the Griess reaction.[19] To measure glutamate, Glutamate Assay Kit colorimetric assay (Yamasa, Tokyo, Japan) was used as described previously.[20]

The mRNA expression of HO-1 was assessed by RT-PCR. Briefly, total RNA was extracted using the guanidinium thiocyanate method (RNeasy Mini Kit; Qiagen, Valencia, CA). cDNAs were generated by RT-PCR using SuperScript II (Invitrogen, Carlsbad, CA) and Ampli TaqDNA polymerase (Applied Biosystems, Branchburg, NJ) in the presence of the specific primers. HO-1 sense, 5'-CTATGTAAAGCGTCTCCA-3'; and HO-1 antisense, 5'-GTCTTTGTGTTCCTCTGTC-3'.

## Measurement of ROS

To measure ROS in neuron-microglia co-cultures, we used the acetate ester form of 2',7'-dichlorofluorescein diacetate ($H_2$DCFDA-AM) probe (Invitrogen). After neuron-microglia co-cultures were treated with or without 100 nmol/L CpG for 3 hours, cells were loaded with dye by replacing media with fresh nerve culture medium containing 5 μmol/L $H_2$DCFDA-AM for 30 minutes. After washing, culture medium containing 5 μmol/L oAβ1-42 was added and the fluorescence of the wells was measured. Fluorescent measurements were made using a Wallac 1420 ARVOMX (PerkinElmer Japan, Yokohama, Japan).

## Immunocytochemistry

Neuronal, microglial, and neuron-microglia co-cultures were fixed with 4% paraformaldehyde for 30 minutes at room temperature, then blocked with 5% normal goat serum in PBS and permeabilized with 0.3% Triton X-100. Neurons were stained with rabbit polyclonal anti-microtubule-associated protein (MAP)-2 antibody (1/500; Chemicon, Temecula, CA) and secondary antibodies conjugated to Alexa 488 (1/1000; Invitrogen). Synthetic Aβ was stained with a mouse monoclonal anti-Aβ antibody (4G8) (1/1000; Chemicon) and secondary antibodies conjugated to Alexa 568 or 647. Microglia were stained with phycoerythrin-conjugated rat anti-mouse CD11b monoclonal antibody (1/300; BD Pharmingen) before fixation. Images were analyzed with a deconvolution fluorescent microscope system (BZ-8000; Keyence, Osaka, Japan). To assess neuronal death induced by Aβ, purified neurons (5 × $10^4$ cells/well) were plated in 24-well multidishes. A total of 5 μM oAβ1-42 or fAβ1-42 was added to the cultures on 13 days in vitro for 24 hours. To assess neuronal death in neuron-microglia co-cultures, 3 hours after treatment with or without TLR ligands, 5 μmol/L oAβ1-42 was added to cultures for 24 hours. Surviving neurons were identified by cytoskeletal morphology of neurons as described previously.[8] Viable neurons stained strongly with an anti-MAP-2 antibody, whereas damaged neurons stained more weakly. The number of MAP-2-positive neurons was counted in representative areas per well. More than 200 neurons were examined in each of five independent trials by a scorer blind to the experimental condition. The number of untreated viable neurons was normalized to 100%.

## Western Blotting

Neuronal cultures were treated with 5 μmol/L oAβ1-42 for 24 hours. Neuron-microglia co-cultures were pretreated with CpG for 3 hours before addition of 5 μmol/L oAβ1-42 for 24 hours. The supernatants of these cultures were collected. oAβ in 10-month-old-Tg 2576 mouse brain was extracted from the soluble, extracellular-enriched fraction as described previously.[21] Hemi-forebrains were harvested in 500 μl of solution containing 50 mmol/L Tris-HCl (pH 7.6), 0.01% Nonidet P-40, 150 mmol/L NaCl, 2 mmol/L EDTA, 0.1% SDS, and protease inhibitor mixture (Sigma-Aldrich, St. Louis, MO). Soluble, extracellular-enriched proteins were collected from mechanically homogenized lysates following centrifugation for 5 minutes at 3000 rpm.

Collected samples were mixed with sample buffer (200 mmol/L Tris-HCl, 8% SDS, and 1% glycerol). Proteins were separated on a 5 to 20% Tris-glycine SDS-polyacrylamide gel and transferred to Hybond-P polyvinylidene difluoride membrane (GE Healthcare UK, Buckinghamshire, UK). Membranes were blocked with 1% skim milk in Tris-buffered saline (TBS) containing 0.05% Tween20 (TBS-T). Blots were incubated in mouse anti-Aβ monoclonal antibody (6E10) (1/1000; Chemicon) diluted in 1% skim milk overnight at 4°C. Subsequently, membranes were washed in TBS-T 3 × 5 minutes and incubated with a horseradish peroxidase-conjugated anti-mouse IgG (1/5000; GE Healthcare) diluted in 1% skim milk for 1 hour. After washing in TBS-T for 1 × 15 minutes, 2 × 5 minutes, and TBS for 1 × 5 minutes, signals were visualized with SuperSignal West Pico Chemiluminescent Substrate (Thermo Fisher Scientific, Rockford, IL). The intensity of the bands was calculated by using CS Analyzer 1.0 (Atto, Tokyo, Japan).

## Novel-Object Recognition Test in oAβ1-42-Induced Cognitive Impairment Mouse Model

oAβ (300 pmol/3 μl), CpG (100 nmol/L), or both oAβ and CpG were ICV injected as described previously.[22,23] The vehicle (PBS) was injected as the control. Briefly, a microsyringe with a 28-gauge stainless-steel needle 3.0 mm long was used for these experiments. C57/BL6 mice were anesthetized lightly with ether, and the needle was inserted unilaterally 1 mm to the right of the midline point equidistant from each eye, at an equal distance between the eyes and the ears and perpendicular to the plane of the skull. A single injection of 3 μl of peptide or vehicle was delivered gradually over 3 minutes. The injection site was confirmed in preliminary experiments. Neither insertion of the needle nor the volume of injection had a significant influence on survival and behavioral responses or cognitive functions.

The novel-object recognition test (NORT) was performed 7 to 8 days after ICV injection of oAβ1-42 or CpG as described previously.[24,25] The experimental apparatus consisted of a plexiglas open-field box (30 × 30 × 35 high cm), with a sawdust-covered floor. The apparatus

was located in a sound-attenuated room and was illuminated with a 60 lux light source. The NORT procedure consisted of three sessions: habituation, training, and retention. Each mouse was individually habituated to the box with 10 minutes of exploration in the absence of objects for 3 consecutive days (habituation session, days 4 to 6). During the training session, two novel objects were symmetrically fixed to the floor of the box, 8 cm from the walls, and each animal was allowed to explore in the box for 10 minutes (day 7). The objects were constructed from a golf ball, wooden column, and wooden triangular pyramid. They were different in shape and color but similar in size. An animal was considered to be exploring the object when its head was facing the object or it was touching or sniffing the object. The time spent exploring each object was recorded. After training, mice were immediately returned to their home cages. During the retention sessions (day 8), the animals were placed back into the same box 24 hours after the training session, but one of the familiar objects used during training had been replaced with a novel object. The animals were then allowed to explore freely for 5 minutes, and the time spent exploring each object was recorded. Throughout the experiments, the objects were used in a counterbalanced manner. A preference index in the retention session, a ratio of the amount of time spent exploring the novel object over the total time spent exploring both objects, was used to measure cognitive function. In the training session, the preference index was calculated as a ratio of the time spent exploring the object that was replaced by the novel object in the retention session over the total time exploring.

## Cued and Contextual Fear-Conditioning Tests in Tg 2576 Mouse Model of AD

Cued and contextual fear conditioning tests were performed at 10 months of age according to previous report,[26] with minor modifications. For measuring basal levels of freezing response (preconditioning phase), mice were individually placed in a neutral cage (a block plexiglas box with abundant wood tips, 30 × 30 × 40 high cm) for 1 minute, then in the conditioning cage (a transparent plexiglas box, 30 × 30 × 40 high cm) for 2 minutes. For training (conditioning phase), mice were placed in the conditioning cage, then a 15-second tone (80 dB) was delivered as a conditioned stimulus. During the last 5 seconds of the tone stimulus, a foot shock of 0.6 mA was delivered as an unconditioned stimulus through a shock generator (Neuroscience Idea). This procedure was repeated four times with 15-second intervals. Cued and contextual tests were performed 1 day after fear conditioning. For the contextual test, mice were placed in the conditioning cage, and the freezing response was measured for 2 minutes in the absence of the conditioned stimulus. For the cued test, the freezing response was measured in the neutral cage for 1 minute in the presence of a continuous-tone stimulus identical to the conditioned stimulus.

Stereotaxic injection was used for these experiments. Mice were anesthetized with sodium pentobarbital (50 mg/kg, i.p.) before stereotaxic implantation of a microinjection cannula into the right lateral ventricle (anteroposterior, −0.3 mm, and mediolateral, +1.0 mm, from the bregma, and dorsoventral, +2.5, from the skull according to the atlas of Franklin and Paxinos).[27] CpG was dissolved in PBS at a concentration of 10 or 100 nmol/L and was injected at a volume of 3 μl for 3 minutes. Same volume of PBS was injected to vehicle mouse. A week after injection, behavioral experiment was performed.

### Immunohistochemistry

Immunohistochemistry was performed on brain tissue of mice after cued and contextual fear-conditioning test. Mice were transcardially perfused with ice-cold borate-buffered 4% paraformaldehyde under deep anesthesia. The brains were rapidly removed after decapitation. Brains were then postfixed overnight in periodate lysine paraformaldehyde, equilibrated in phosphate buffered 20% sucrose for 48 hours, and embedded into Tissue-Tek OCT compound (Sakura Finetechnical, Tokyo, Japan) and frozen at −80°C overnight. Coronal brain sections (20 μm) were cut with a cryostat. The sections were permeabilized with 1% Triton X-100 after blocking with 10% normal goat serum for 30 minutes. The cell nucleus was stained with Hoechst 33342 (1 μg/ml; Invitrogen). Aβ was stained with mouse monoclonal anti-Aβ antibody (4G8) (1/1000; Chemicon) and secondary antibodies conjugated to Alexa 488. Microglia were stained with a rat anti-mouse CD11b monoclonal antibody (1/1000; AbD Serotec, Oxford, UK) and secondary antibodies conjugated to Alexa 568. Images were collected and analyzed with a deconvolution fluorescent microscope system. Aβ load in immunostained tissue sections were quantified using BZ-analyzer (Keyence) as reported previously.[28] Seven sections were analyzed per animal. Total Aβ burden was quantified for the cortex and for the hippocampus on coronal plane sections stained with the monoclonal antibody 4G8. The cortical area was dorsomedial from the cingulate cortex and extended ventrolaterally to the rhinal fissure within the right hemisphere. Test areas (640 μm × 480 μm) were randomly selected. Total Aβ burden was calculated as the percentage of test area occupied by Aβ. Hippocampal measurements (600 × 600 μm) were performed similarly to the cortical analysis.

### Statistical Analysis

Statistical significance of the biochemical experiments and the behavioral data were assessed with one-way analysis of variance, followed by post hoc Tukey test or Newman-Keuls test using GraphPad Prism version 5.0 (GraphPad Software, La Jolla, CA).
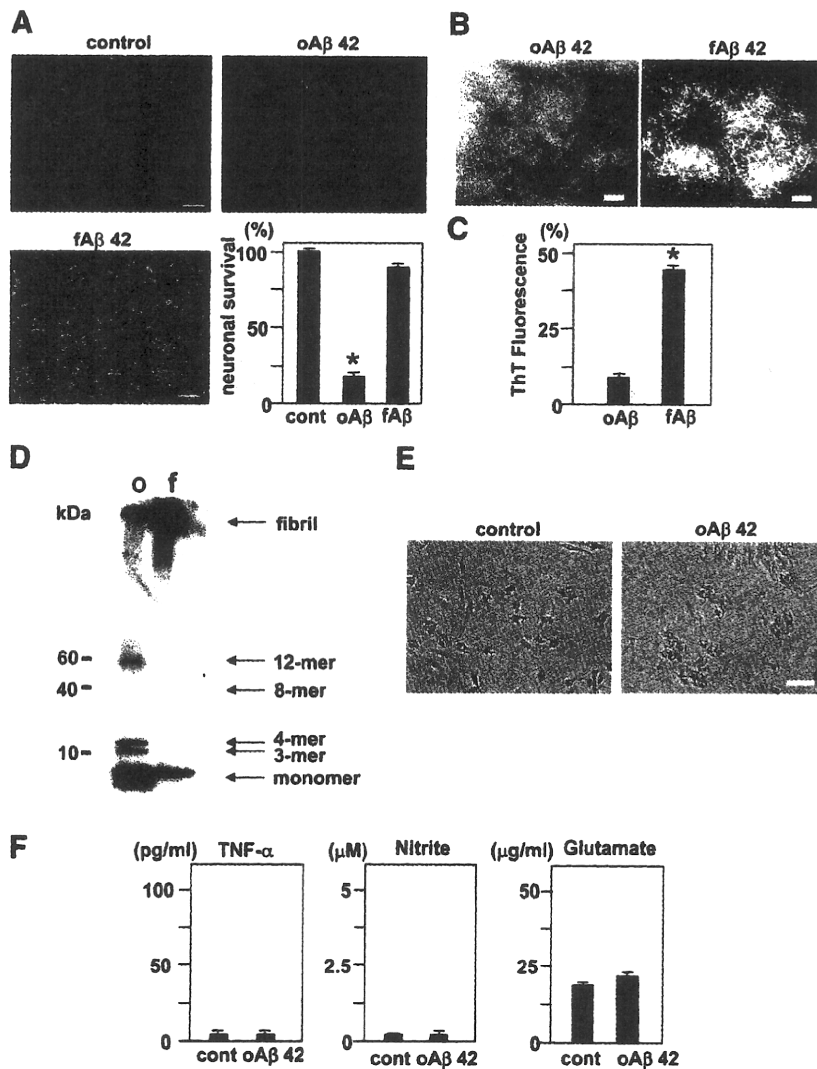
**Figure 1.** Neurotoxicity and morphologies of oAβ1-42 and fAβ1-42, and microglial response to oAβ1-42. **A:** The evaluation of neurotoxicity induced by oAβ1-42 and fAβ1-42. Neuronal cultures were treated with 5 μmol/L oAβ1-42 or fAβ1-42 for 24 hours. Neurons were stained with an anti-MAP-2 antibody (green). Aβ was stained with a mouse anti-amyloid β protein monoclonal antibody (4G8) (red). oAβ1-42 exhibited more striking neurotoxicity than fAβ1-42. Scale bar, 50 μm. Neuronal survival rate in oAβ1-42 treatment significantly decreased. *P < 0.05 as compared with the rate in control cultures. Each column indicates the mean ± SEM (n = 5). **B:** Images of oAβ1-42 (**left**) and fAβ1-42 (**right**) collected with an electron microscope. Scale bar, 100 nm. **C:** Thioflavin T assay for oAβ1-42 and fAβ1-42. *P < 0.05 as compared with the value of oAβ1-42. **D:** Western blot analysis of oAβ1-42 and fAβ1-42. oAβ1-42 (o) contained monomers, small oligomeric trimers (3-mer) and tetramers (4-mer), and the larger oligomers (octamers (8-mer) and dodecamers (12-mer)), whereas fAβ1-42 (f) contained monomers and fibrils. **E:** Microglial cultures were treated with or without 5 μmol/L oAβ1-42 for 24 hours. In a phase contrast, oAβ1-42 induced microglial adhesion. Scale bar, 50 μm. **F:** The measurement of TNF-α (**left**), nitrite (**middle**), and glutamate (**right**) produced by microglia activated with oAβ1-42. Microglial cultures were treated with 5 μmol/L oAβ1-42 for 24 hours. Each column indicates the mean ± SEM (n = 7).

## Results

### Neurotoxicity of oAβ1-42

First, we investigated the toxic effects of oAβ and fAβ on primary cortical neurons. Administration of 5 μmol/L oAβ1-42 to cortical cultures on DIV 13 for 24 hours resulted in significant neuronal death. The network of MAP-2-positive dendrites collapsed and neuronal survival decreased to 20% (Figure 1A). In contrast, administration of fAβ1-42 did not induce neuronal cell death, although Aβ deposition was observed on dendrites (Figure 1A). Thus, oAβ1-42 exhibits a more potent neurotoxicity than fAβ1-42. Both oAβ1-40 and fAβ1-40 did not induce neuronal cell death (Supplemental Figure S1, see http://ajp.amjpathol.org). We evaluated the morphology of oAβ1-42 and fAβ1-42 by transmission electron microscopy. We observed fine spherical particles of oAβ1-42 and fibril formation by fAβ1-42 (Figure 1B). The fluorescence of Thioflavin T, a marker for amyloid fibril formation, was associated with fAβ1-42 (Figure 1C). Western blotting

with an antibody directed against Aβ (6E10) revealed that a solution of oAβ1-42 contained monomers, trimers (3-mer), tetramers (4-mer), and larger oligomers (octamers (8-mer) and dodecamers (12-mer)). In contrast, a solution of fAβ1-42 contained monomers and fibrils, but not oligomers (Figure 1D).

In primary microglial culture, administration of 5 μmol/L oAβ1-42 for 24 hours induced microglial adhesion (Figure 1E), but did not induce the production of neurotoxic mediators such as TNF-α, glutamate, or nitrite, a stable breakdown product of NO (Figure 1F).

### Microglia Activated with CpG Attenuate the Neurotoxicity Induced by oAβ1-42

To define the role of microglia in the neurotoxicity of oAβ1-42, we evaluated neuronal survival in neuron-microglia co-cultures. Neurons stained with anti-MAP-2 antibody exhibited no detectable morphological abnormalities and possessed intact cell bodies and dendrites, and
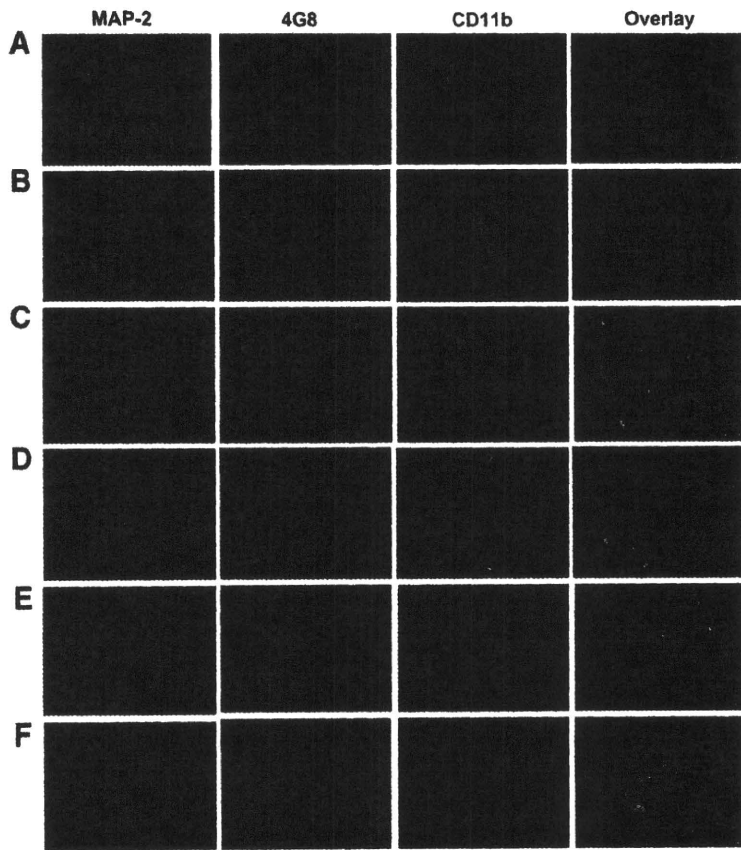
| MAP-2 | 4G8 | CD11b | Overlay |
|---|---|---|---|



**Figure 2.** Protective effect of microglia activated with CpG against oAβ1-42 neurotoxicity. **A:** Representative deconvolution fluorescent images of control neuron-microglia co-cultures (1:2 of neuron: microglia). **B:** Neuronal cultures treated with 5 μmol/L oAβ1-42. **C:** Neuron-microglia co-cultures (1:2 neuron to microglia) treated with oAβ1-42. **D:** Neuron-microglia co-cultures stimulated with 1 nmol/L CpG and oAβ1-42 (**E**) or with 10 nmol/L CpG and oAβ1-42 (**F**) or with 100 nmol/L CpG and oAβ1-42. After 3 hours of treatment with CpG, cultures were treated with oAβ1-42 for 24 hours. Neurons were stained with an anti-MAP-2 antibody (green). Aβ was stained with 4G8 (red) and microglia were stained with a phycoerythrin-conjugated anti-CD11b antibody (blue). Scale bar, 50 μm. **G:** Neuronal survival rate was quantified as the percentage of intact neurons following treatment relative to control wells. The viability of untreated neurons (control) was normalized to 100%. *$P < 0.05$ as compared with the survival rate of neuron-microglia co-cultures treated with oAβ1-42. Each column indicates the mean ± SEM ($n = 7$).

microglia stained with anti-CD11b antibody were also intact in unstimulated co-cultures (Figure 2A). After treatment of neuronal cultures with 5 μmol/L oAβ1-42 for 24 hours, the neuronal cells were severely damaged, and the survival rate decreased to 18% (Figure 2, B and G). Similarly, the neuronal survival rate was not improved in neuron-microglia co-cultures treated with oAβ1-42 (Figure 2, C and G), which implies that unstimulated microglia have not protective effect against oAβ1-42 neurotoxicity. Administration of CpG to neuronal cultures or neuron microglia co-cultures induced no toxic change (Supplemental Figure S2A, see *http://ajp.amjpathol.org*). After 3 hours of treatment with 1 nmol/L, 10 nmol/L, or 100 nmol/L CpG, 5 μmol/L oAβ1-42 was added to neuron-microglia co-cultures for 24 hours. The neuroprotective effect was not evident in culture with 1 nmol/L CpG (Figure 2, D and G). However, microglia treated with 10 or 100 nmol/L CpG prevented neuronal cell death, and the neuronal survival rate was significantly improved reaching 53 and 62%, respectively (Figure 2, E–G). In neuronal cultures, CpG did not attenuate the neurotoxicity induced by oAβ1-42 (Figure 2G). Moreover, 100 nmol/L CpG attenuated oAβ1-42-induced neurotoxicity for 48 hours, whereas other TLR ligands such as peptidoglycan and lipopolysaccharide did not (Supplemental Figure S2B, see *http://ajp.amjpathol.org*). We conclude from these findings that CpG-activated microglia have neuroprotective effect against oAβ1-42 neurotoxicity *in vitro*.

## CpG-Activated Microglia Increase the Clearance of oAβ1-42, Produce the Antioxidant Enzyme HO-1 and Aβ-Degrading Enzyme MMP-9, and Release Fewer Neurotoxic Molecules

To elucidate the mechanisms of neuroprotection by microglia activated with CpG, we examined whether CpG increased the clearance of oAβ1-42. Western blot analysis revealed that there was no significant difference between the amount of oAβ1-42 present in the supernatants of neuronal cultures and in neuron-microglia co-cultures without CpG administration. (Figure 3A). However, CpG dose-dependently decreased the amount of oAβ1-42 in neuron-microglia co-cultures, especially treatment with 100 nmol/L CpG significantly decreased the amount of 3-, 4-, 8-, and 12-mer of oAβ1-42 (Figure 3, B and C). Moreover, we examined the effect of CpG on Aβ uptake by microglia alone at 1 and 24 hours time points. We found that CpG significantly enhanced microglial uptake of oAβ at both 1 and 24 hours (Supplemental Figure S3A, see *http://ajp.amjpathol.org*).

Because oxidative stress is a major component of oAβ1-42 neurotoxicity, we examined whether microglia activated with CpG express the antioxidant enzyme HO-1. CpG-activated microglia produced HO-1 in a dose-dependent manner. A total of 10 and 100 nmol/L CpG significantly increased the production of HO-1. The
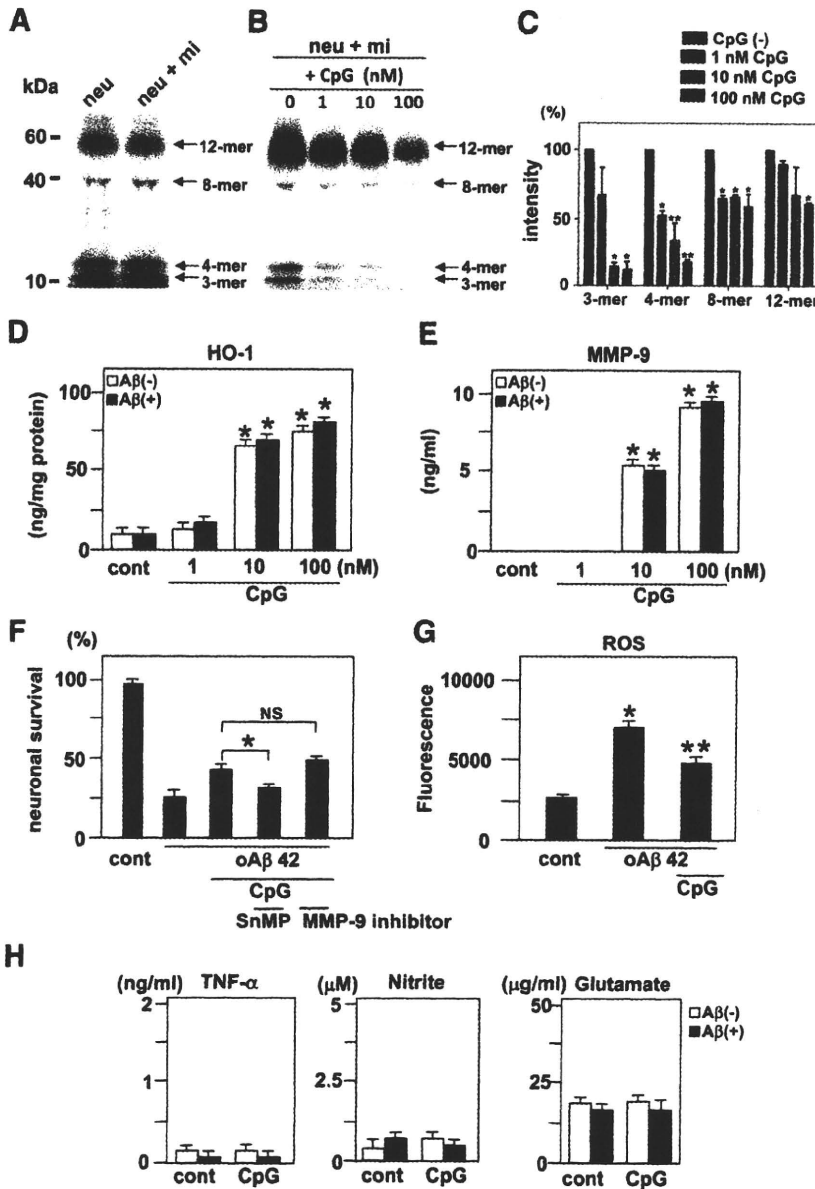
**Figure 3.** Clearance of oAβ1-42 and the production of HO-1, MMP-9, and neurotoxic molecules by microglia activated with CpG. **A:** Western blot analysis of oAβ1-42 in neuronal cultures (neu) and neuron-microglia co-cultures (neu + mi). Twenty-four hours after addition of 5 μmol/L oAβ1-42, oAβ1-42 present in the supernatants of these cultures was detected by Western blotting. **B:** Western blot analysis of oAβ1-42 in neuron-microglia co-cultures with CpG treatment. Neuron-microglia co-cultures (neu + mi) were treated with 5 μmol/L oAβ1-42 for 24 hours following 3 hours of treatment with 1, 10, or 100 nmol/L CpG. Microglia activated with CpG dose-dependently reduced the amount of oAβ1-42 in the supernatants. **C:** Semiquantification of oAβ1-42 in **B** by densitometric analysis. The amount of oAβ1-42 in neuron-microglial co-cultures without CpG (black) was normalized to 100%. oAβ1-42 in co-cultures treated with 1 nmol/L CpG (blue), 10 nmol/L CpG (green), or 100 nmol/L CpG (red) was calculated. $^*P < 0.05$ and $^{**}P < 0.01$ as compared with the intensity of oAβ1-42 in neuron-microglia co-cultures without CpG. Each column indicates the mean ± SEM ($n = 6$). The production of HO-1 (**D**) and MMP-9 (**E**) by microglia activated with CpG in the absence or presence of oAβ1-42. After 3 hours of treatment with CpG, microglial cultures were treated with or without oAβ1-42 for 24 hours. $^*P < 0.05$ as compared with untreated controls. Each column indicates the mean ± SEM ($n = 3$–5). **F:** The effect of HO-1 and MMP-9 on oAβ1-42 neurotoxicity. Neuron-microgila co-cultures were treated with 100 nmol/L CpG in the presence of 10 μmol/L tin-mesoporphyrin (SnMP) IX, a specific HO-1 inhibitor, or 50 nmol/L MMP-9 inhibitor for 3 hours, and then oAβ1-42 was added to the cultures for 24 hours. Tin-mesoporphyrin IX, but not the MMP-9 inhibitor, decreased neuronal survival rate. $^*P < 0.05$ as compared with CpG-treated cultures without inhibitors. Each column indicates the mean ± SEM ($n = 6$–9). **G:** The suppressive effect of CpG on ROS production by oAβ in the neuron microglia co-cultures. After neuron-microglia co-cultures were treated with or without 100 nmol/L CpG for 3 hours, cells were loaded with fresh nerve culture medium containing 5 μmol/L H₂DCFDA-AM for 30 minutes. After washing, culture medium containing 5 μmol/L oAβ1-42 was added and the increment of the fluorescence was calculated at 5 minutes. $^*P < 0.05$ as compared with untreated controls. $^{**}P < 0.05$ as compared with co-culture cells treated with oAβ1-42. Each column indicates the mean ± SEM ($n = 4$). **H:** The measurement of TNF-α (**left**), nitrite (**middle**), and glutamate (**right**) produced by microglia activated with 100 nmol/L CpG with or without oAβ1-42. After 3 hours treatment with CpG, microglial cultures were treated with or without oAβ1-42 for 24 hours. $^*P < 0.05$ as compared with untreated microglia. Each column indicates the mean ± SEM ($n = 7$).

production levels were not influenced by exposure to oAβ1-42 (Figure 3D). Since the anti-inflammatory cytokine IL-10 induces HO-1 expression by macrophages,[29] we also examined and confirmed that IL-10 induced HO-1 mRNA expression by microglia (Supplemental Figure S3B, see http://ajp.amjpathol.org). Although CpG induced IL-10 in microglia, the expression was suppressed by oAβ1-42 treatment (Supplemental Figure S3C, see http://ajp.amjpathol.org).

MMP-9 is also thought to play a neuroprotective role in AD because it degrades both oAβ and fAβ. A total of 10 and 100 nmol/L CpG significantly induced MMP-9 pro-

duction in microglia with or without treatment of oAβ1-42 (Figure 3E). To determine whether HO-1 and MMP-9 contribute to the neuroprotective effects of CpG-activated microglia, we applied the specific HO-1 inhibitor tin-mesoporphyrin IX (Frontier Scientific, Logan, UT) and MMP-9 inhibitor (Merck, Darmstadt, Germany). The neuroprotective effect of CpG was abolished by treatment with 10 μmol/L tin-mesoporphyrin IX (Figure 3E). However, inhibition of MMP-9 with an MMP-9 inhibitor at 50 nmol/L did not influence the neuroprotective effect of CpG-activated microglia (Figure 3F). These results imply that HO-1 rather than MMP-9 may contribute to the
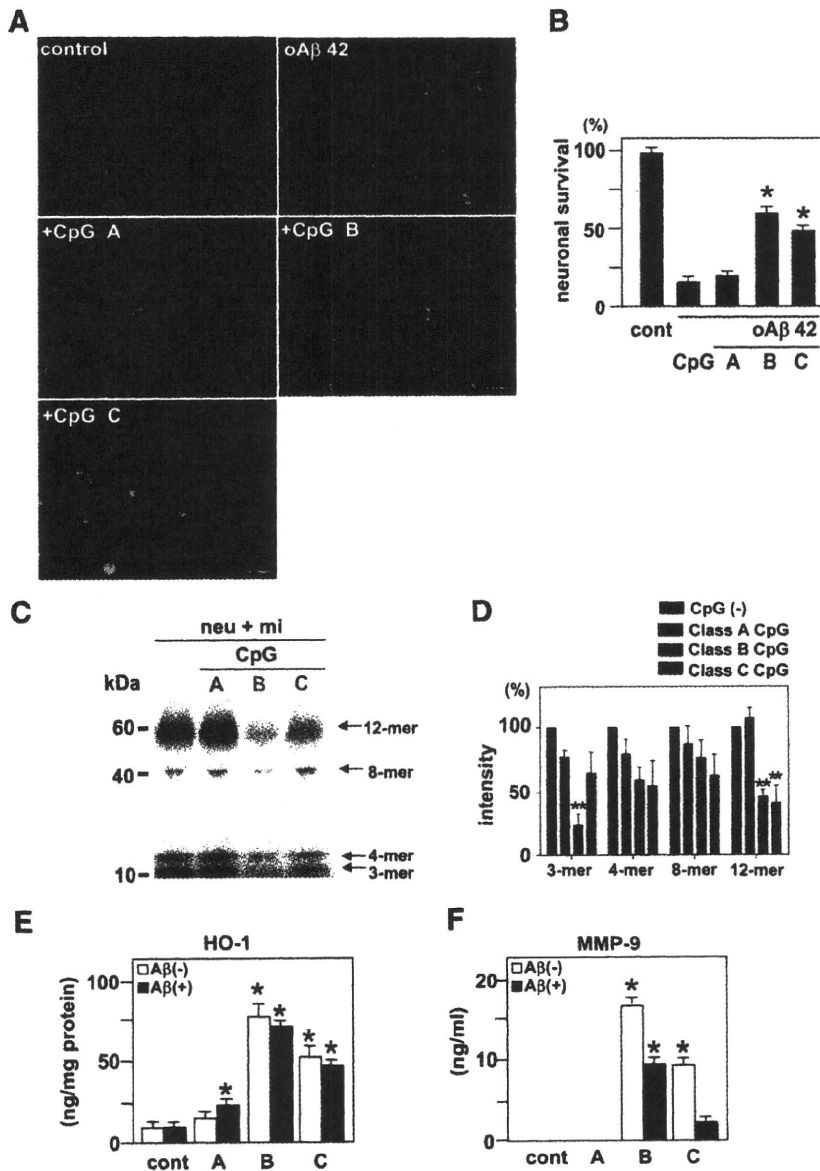
**Figure 4.** Protective effect of microglia activated with each subclass of CpG against oAβ1-42 neurotoxicity. **A:** Class B and class C, but not class A, CpGs exhibited neuroprotective effects against oAβ1-42 neurotoxicity in neuron-microglia co-cultures. After 3 hours incubation with 100 nmol/L class A, class B, or class C CpGs, oAβ1-42 was added to neuron-microglia co-cultures for 24 hours. Neurons were stained with anti-MAP-2 antibody (green). Aβ was stained with 4G8 (red), and microglia were stained with anti-CD11b antibody (blue). Scale bar, 50 μm. **B:** Neuronal survival rate was quantified. The viability of neurons in untreated co-cultures (control) was normalized to 100%. *$P < 0.05$ as compared with the co-cultures treated with oAβ1-42 alone. Each column indicates the mean ± SEM ($n = 7$). **C:** Western blot analysis of oAβ1-42 in neuron-microglia co-cultures with subclassese of CpG treatment. Neuron-microglia co-cultures (neu + mi) were treated with 5 μmol/L oAβ1-42 for 24 hours following 3 hours of treatment with 100 nmol/L class A, class B, or class C CpGs. Microglia activated with class B or class C CpGs reduced the amount of oAβ1-42 in the supernatants. **D:** Semiquantification of oAβ1-42 in **C** by densitometric analysis. The amount of oAβ1-42 in neuron-microglial co-cultures without CpG (black) was normalized to 100%. oAβ1-42 in co-cultures treated with class A CpG (blue), class B CpG (green), or class C CpG (red) was calculated. **$P < 0.01$ compared with the intensity of oAβ1-42 in neuron-microglia co-cultures without CpG. Each column indicates the mean ± SEM ($n = 7$). The production of HO-1 (**E**) and MMP-9 (**F**) by microglia activated with subclasses of CpG in the absence or presence of oAβ1-42. After 3 hours incubation with 100 nmol/L class A, class B, or class C CpGs, microglial cultures were treated with or without oAβ1-42 for 24 hours. *$P < 0.05$ as compared with untreated control cultures. Each column indicates the mean ± SEM ($n = 3$–5).

neuroprotection of CpG. Furthermore, treatment of oAβ significantly increased ROS production in the neuron microglia co-cultures. Pretreatment of 100 nmol/L CpG significantly suppressed ROS production by oAβ (Figure 3G).

Although TLR4 ligand lipopolysaccharide generally increases microglial production of neurotoxic molecules including TNF-α, nitrite and glutamate; 100 nmol/L CpG did not induce these toxic molecules in microglia (Figure 3H).

## Microglia Activated with Class B and C, but not Class A CpG, Attenuate oAβ1-42 Neurotoxicity

CpG ODNs are divided into three classes by their ability to induce IFN-α expression in plasmacytoid dendritic cells (class A) and to promote survival, activation, and maturation of B cells and plasmacytoid dendritic cell

(class B) or both (class C)[30]. We examined which class of CpG induces the neuroprotective effects of microglia. Class A CpG neither activated microglia nor induced neuroprotective effects against oAβ1-42 toxicity, whereas both class B and C CpGs activated microglia and significantly increased neuronal survival, to 58 and 49% following oAβ1-42 treatment, respectively (Figures 4, A and B). Western blot analysis revealed that class B CpG significantly decreased the amount of trimers and dodecamers of oAβ1-42 present in the supernatants of neuron-microglia co-cultures, and class C CpG significantly decreased dodecamers of oAβ1-42, whereas oAβ1-42 did not decrease by the administration of class A CpG (Figure 4, C and D). In addition, microglia activated with class B and C CpGs expressed HO-1 in both the absence or presence of oAβ1-42, whereas treatment with class A CpG only slightly increased HO-1 expression in the pres-
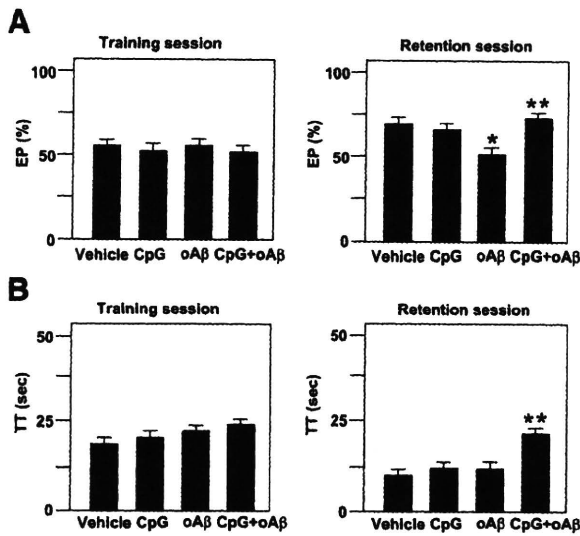
**A**

Training session

Retention session



**B**

Training session

Retention session



**Figure 5.** Effect of ICV injection of CpG on oAβ1-42-induced cognitive impairment in the NORT. **A:** Exploratory preference (EP) and total exploring time (TT) (**B**) in the training session (**left**) and the retention session (**right**). NORT was performed 7 to 8 days after ICV injection of oAβ1-42. Each column indicates the mean ± SEM ($n$ = 6-7). $^*P$ < 0.05 as compared with controls. $^{**}P$ < 0.05 as compared with oAβ1-42-injected mice.

ence of oAβ1-42 (Figure 4E). Microglia activated with class B and C CpGs also produced MMP-9 (Figures 4F).

## ICV Injection of CpG Ameliorates oAβ-Induced Impairment of Recognition Memory in the NORT

To examine the role of CpG-activated microglia in cognitive dysfunction induced by oAβ1-42, we investigated the effect of in vivo administration of CpG on the impairment of recognition memory in the NORT after ICV injection of oAβ1-42. Mice injected with oAβ1-42 displayed significantly reduced exploratory preference for the novel object in the retention session ($F_{(3,21)}$ = 3.68, $P$ < 0.05; Figure 5A), although total exploration time in the training and retention sessions was unaffected. The result implies that oAβ1-42 induces the impairment of recognition memory. Simultaneous injection of CpG with oAβ1-42 significantly improved both exploratory preference ($F_{(3,21)}$ = 3.68, $P$ < 0.05; Figure 5A) and total exploration time ($F_{(3,21)}$ = 4.41, $P$ < 0.05; Figure 5B) in the retention session, although exploratory preference and total exploration time were unaffected in the training session.

## ICV Injection of CPG Ameliorates the Impairment of Associative Learning in the Cued and Contextual Fear-Conditioning Tests in Tg2576 Mice

Next, we examined the effect of CpG on the cognitive function of Tg2576 mouse model of AD. We evaluated associative learning at the age of 10 months in a conditioned fear learning test. In the preconditioning phase (training), the mice hardly showed any freezing response. There were no differences in basal levels of freezing

response between the groups (data not shown). In the contextual learning test, wild-type mice showed a marked contextual freezing response 24 hours after fear conditioning (Figure 6A). However, vehicle-injected Tg2576 mice exhibited less of a freezing response in the contextual tests (Figure 6A), indicating an impairment of associative learning. The CpG (10 or 100 nmol/L)-injected Tg2576 mice were indistinguishable from wild-type mice, and the CpG treatment dose-dependently and significantly reversed the contextual freezing response as compared with vehicle-injected Tg2576 mice ($F_{(3,35)}$ = 9.54, $P$ < 0.05; Figure 6A). In the cued (tone) learning test, although there was no significant difference in the cued freezing response at 24 hours after fear conditioning between wild-type and vehicle-injected Tg2576 mice, both injection of 10 and 100 nmol/L CpG showed a tendency to reverse the cued freezing response (Figure 6B). No alterations of nociceptive response were found in any of the mutant mice: there was no difference in the minimal current required to elicit flinching/running, jumping, or vocalization among the mice (data not shown). Then, we examined whether CpG decreased Aβ deposits in the cortex (Figure 6C) and the hippocampus (Figure 6D) of Tg 2576 mice. No Aβ deposits were seen in wild-type mice. Although Aβ deposits (green) were abundant in the cortex and the hippocampus of vehicle-injected Tg2576 mice, ICV injection of CpG significantly decreased Aβ deposits in both areas. Microglia (red) clustered around Aβ deposits (Figure 6, C and D). CpG decreased Aβ load in a significant, dose-dependent manner in both areas (Figure 6E). We examined oAβ in the soluble, extracellular-enriched fractions of the hemi-forebrains of mice and detected 12-mer oAβ in vehicle-injected Tg2576 mice by Western blotting. The 12-mer oAβ was strikingly and significantly decreased in 100 nmol/L CpG-injected Tg2576 mice (Figure 6, F and G).

## Discussion

Recent studies have proposed that oAβ1-42 contributes to the neurotoxicity associated with AD. AD begins with subtle alterations of hippocampal synaptic efficacy before frank neuronal degeneration, and this synaptic dysfunction is caused by diffusible oAβ.[31] Disruption of hippocampal long-term potentiation and synaptic plasticity by oAβ1-42 appears to involve $Ca^{2+}$ signaling,[32] oxidative stress mediated by an N-methyl-D-aspartate receptor,[4,33] and protein phosphatase 1.[34] In addition, oAβ interferes with insulin receptor function in hippocampal neurons and inhibits the activation of specific kinases required for long-term potentiation.[35] In the present study, we have confirmed that oAβ1-42 exhibits more potent neurotoxicity than fAβ1-42 in murine cortical cultures.[5,36] Therefore, decreasing or preventing formation of oAβ1-42 is a potential therapeutic strategy against AD.

The precise role of microglia in oAβ1-42 toxicity remains unclear. Microglia stimulated with Aβ are reported to release proinflammatory cytokines via the nuclear factor κB[37,38] and contribute to the pathogenesis of AD. However, in our experimental conditions, oAβ1-42 neither
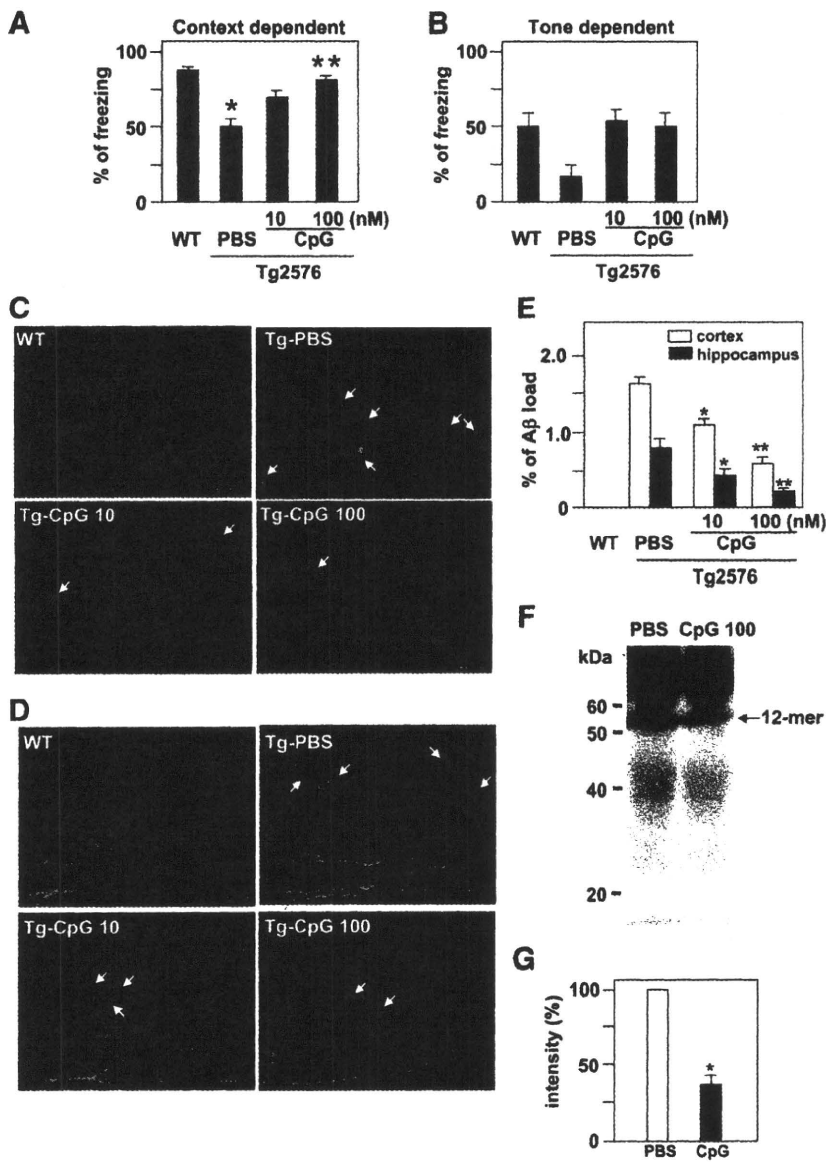
**Figure 6.** Effect of ICV injection of CpG on associative learning in the cued and contextual conditioning tests and Aβ clearance in Tg2576 mice. The retention session was performed 24 hours after the training. Context-dependent (**A**) and tone-dependent (**B**) freezing times were measured at the age of 10 months. Each column indicates the mean ± SEM (wild-type (WT) mice, $n = 14$; vehicle-treated (PBS) Tg2576 mice, $n = 9$; CpG (10 nmol/L)-treated Tg2576, $n = 8$; CpG (100 nmol/L)-treated Tg2576, $n = 8$). $^*P < 0.05$ compared with wild type. $^{**}P < 0.05$ as compared with vehicle-treated Tg2576 mice. **C:** Aβ deposits in the cortex. Aβ was stained with 4G8 (green), microglia stained with anti-CD11b antibody (red), and cell nucleus stained with Hoechst 33342 (blue). **White arrows** indicate Aβ deposits surrounding by microglia. Scale bar, 200 μm. **D:** Aβ deposits in the hippocampus. Scale bar, 200 μm. **E:** Quantification of Aβ deposits in **C** and **D**. The ratio between the Aβ deposits area and the total area of the analyzed region was multiplied by 100. $^*P < 0.05$ and $^{**}P < 0.01$ as compared with vehicle-treated Tg2576 mice. Each column indicates the mean ± SEM ($n = 3$). **F:** Western blot analysis of oAβ extracted from the hemi-forebrains of Tg 2576 mice. A 12-mer oAβ was detected in vehicle-treated Tg2576 mice and decreased in 100 nmol/L CpG-injected Tg2576 mice. **G:** Semi-quantification of 12-mer oAβ by densitometric analysis. The amount of 12-mer oAβ1-42 in vehicle-treated Tg2576 mice was normalized to 100%. $^*P < 0.05$ as compared with vehicle-treated Tg2576 mice. Each column indicates the mean ± SEM ($n = 4$).

activated microglia nor induced the release of neurotoxic proinflammatory cytokines, NO, or glutamate. These results suggest that oAβ1-42 is not acting to trigger of microglial neurotoxicity.

TLR signaling pathways contribute to phagocytosis of Aβ. TLR2 acts as an endogenous receptor for the clearance of Aβ by bone marrow-derived microglia.[9] Interestingly, a TLR4 mutation exacerbates Aβ burden in mouse models of AD.[39] Thus, we investigated whether microglia activated with TLR ligands exert neuroprotective effects against oAβ1-42 toxicity. Consequently, we found that TLR9 ligand CpG enhanced microglial neuroprotection. Furthermore, CpG exerted the neuroprotective effect of BV-2 microglial cell line against oAβ toxicity (data not shown). TLR9, which detects single-stranded DNA containing unmethylated CpG, is located in intracellular endosomal-lysosomal compartment. We confirmed that microglia expressed TLR9 at a higher level, whereas

astrocytes and neuronal cells expressed it at a lower level (data not shown). Thus, CpG mainly acts on microglia in the central nervous system. TLR7 and TLR8 are closely associated with TLR9. They are also located in endosomal-lysosomal compartment and detect single-stranded RNA. The ligands for TLR7 and TLR8 may also have some roles in microglial neuroprotection.

Western blot analysis revealed that microglia activated with CpG reduced the amount of oAβ present in the supernatant of treated cultures. Moreover, CpG was a potent inducer of antioxidant enzyme HO-1. The up-regulation of HO-1 in microglia by CpG treatment may lead to neuroprotection via suppression of ROS production by oAβ. HO-1, a member of the heat-shock protein family, is a microsomal enzyme that oxidatively cleaves heme to produce biliverdin, carbon monoxide, and iron.[40] Aβ binds to heme to promote a functional heme deficiency, mitochondrial dysfunction, and neurotoxicity.[41] Amyloid

precursor protein also binds to HO, and oxidative neurotoxicity is markedly enhanced in cerebral cortical cultures from amyloid precursor protein Swedish mutant transgenic mice.[42]

HO-1 is reported to be induced by the anti-inflammatory cytokine IL-10.[29] Although CpG induced IL-10 in microglia in the absence of oAβ, IL-10 production was inhibited in the presence of oAβ. Therefore, HO-1 may be induced by a discrete mechanism independent from IL-10 in AD.

MMP-9, a protease that degrades Aβ, is expressed at higher levels in the brains of AD patients and may play an important role in amyloid clearance by degrading both oAβ and fAβ.[10] MMP-9 expression is increased by serum amyloid A through formyl peptide receptor-like-1.[43] Although CpG stimulation induced MMP-9 in microglia, inhibiting MMP-9 pharmacologically did not affect neuroprotection by microglia. Thus, MMP-9 may not mainly contribute to the neuroprotection provided by CpG-activated microglia.

In the present study, CpG induced fewer neurotoxic molecules such as TNF-α, NO, and glutamate in microglia, whereas previous studies have reported that CpG-activated microglia produce TNF-α, IL-12, and NO[44] and induce neuronal damage.[45] The discrepancies between these studies and our experiments may be a consequence of differences in the concentrations of TLR ligands used. Higher concentration (10 μmol/L) of CpG have been used for microglial activation in previous reports, whereas here we have used lower concentrations (1 to 100 nmol/L) of CpG.

In addition, we observed that the neuroprotective effect differs among CpG ODN classes. The responses of microglia to the different classes of CpG have not been fully understood. Here, we showed for the first time that class A CpG did not activate microglia, whereas class B and C CpGs induced neuroprotection by microglia that was mediated by clearance of oAβ and induction of HO-1. Three major classes of CpG ODN are structurally distinct. The structures of class A CpG include poly-G motifs at the 5′ and/or 3′ ends that are capable of forming very stable but complex higher-ordered structures and a central phosphodiester region containing one or more CpG motifs in a self-complementary palindrome. Class B CpG has a completely phosphorothioate backbone and does not form typically higher-ordered structures. Class C CpG has a phosphorothioate backbone, and 3′ palindrome forms duplex.[46] These distinct structures of CpG ODN may reflect different microglial responses.

Finally, we examined the effect of CpG on oAβ1-42 neurotoxicity in two different *in vivo* studies. The ICV administration of Aβ25-35 is reported to cause cognitive impairment in a NORT. Oxidative stress contributes to the onset of this cognitive dysfunction.[23] We found that injection of oAβ1-42 also induced cognitive impairment as assessed by NORT. Surprisingly, one-time ICV injection of CpG improved both the cognitive impairment by oAβ1-42 in NORT. The impairment of associative learning in Tg 2576 mouse model of AD was also effectively suppressed by ICV injection of CpG. We also confirmed that CpG treatment decreased Aβ deposits and oAβ in

Tg 2576 mice. Our results concur with the recent study that a total of 14 i.p. injection of CpG into Tg 2576 mice beginning at the age of 6 weeks, and once a month, ameliorates AD-related pathology.[28] Aβ plaques are reported to form extraordinarily quickly, over 24 hours. Within 1 to 2 days of a new plaque's appearance, microglia are activated and recruited to the site.[47] ICV injection of CpG may directly induce microglial activation via TLR9 and enhance microglial rapid uptake of oAβ through fluid-phase macropinocytosis as reported recently.[48] CpG may also enhance microglial phagocytosis of fAβ through formyl peptide receptor-like 2.[11] Such mechanisms of Aβ clearance by CpG can decrease Aβ plaque formation in Tg 2576 mice.

Recently, the therapeutic potential of CpG has generated great interest.[46] CpG offers a potent adjuvant activity that elicits a more effective immune response to infectious agents or tumors. A previous report[49] demonstrated that CpG strongly inhibits the effector phase of inflammatory arthritis. In addition, CpG can serve as a potent preconditioning stimulus and provide protection against ischemic brain injury.[50] Our findings suggest that CpG, especially class B and C, may also be effective therapeutic agents against oAβ1-42 neurotoxicity in AD.

## References

1. Busciglio J, Lorenzo A, Yeh J, Yankner BA: β-Amyloid fibrils induce tau phosphorylation and loss of microtubule binding. Neuron 1995, 14:879–888

2. Grace EA, Rabiner CA, Busciglio J: Characterization of neuronal dystrophy induced by fibrillar amyloid β: implications for Alzheimer's disease. Neuroscience 2002, 114:265–273

3. Walsh DM, Klyubin I, Fadeeva JV, Cullen WK, Anwyl R, Wolfe MS, Rowan MJ, Selkoe DJ: Naturally secreted oligomers of amyloid β protein potently inhibit hippocampal long-term potentiation in vivo. Nature 2002, 416:535–539

4. De Felice FG, Velasco PT, Lambert MP, Viola K, Fernandez SJ, Ferreira ST, Klein WL: Aβ oligomers induce neuronal oxidative stress through an N-methyl-D-aspartate receptor-dependent mechanism that is blocked by the Alzheimer drug memantine. J Biol Chem 2007, 282:11590–11601

5. Deshpande A, Mina E, Glabe C, Busciglio J: Different conformations of amyloid β induce neurotoxicity by distinct mechanisms in human cortical neurons. J Neurosci 2006, 26:6011–6018

6. Meda L, Cassatella MA, Szendrei GI, Otvos L Jr, Baron P, Villalba M, Ferrari D, Rossi F: Activation of microglial cells by β-amyloid protein and interferon γ. Nature 1995, 374:647–650

7. McGeer PL, McGeer EG: Inflammation, autotoxicity and Alzheimer disease. Neurobiol Aging 2001, 22:799–809

8. Mizuno T, Kurotani T, Komatsu Y, Kawanokuchi J, Kato H, Mitsuma N, Suzumura A: Neuroprotective role of phosphodiesterase inhibitor Ibudilast on neuronal cell death induced by activated microglia. Neuropharmacology 2004, 46:404–411

9. Richard KL, Filali M, Préfontaine P, Rivest S: Toll-like receptor 2 acts as a natural innate immune receptor to clear amyloid β 1-42 and delay the cognitive decline in a mouse model of Alzheimer's disease. J Neurosci 2008, 28:5784–5793

10. Yan P, Hu X, Song H, Yin K, Bateman RJ, Cirrito JR, Xiao Q, Hsu FF, Turk JW, Xu J, Hsu CY, Holtzman DM, Lee JM: Matrix metalloproteinase-9 degrades amyloid-β fibrils in vitro and compact plaques in situ. J Biol Chem 2006, 281:24566–24574

11. Iribarren P, Chen K, Hu J, Gong W, Cho EH, Lockett S, Uranchimeg B, Wang JM: CpG-containing oligodeoxynucleotide promotes microglial cell uptake of amyloid β 1-42 peptide by up-regulating the expression of the G-protein-coupled receptor mFPR2. FASEB J 2005, 19:2032–2034

12. Chen K, Iribarren P, Hu J, Chen J, Gong W, Cho EH, Lockett S, Dunlop NM, Wang JM: Activation of Toll-like receptor 2 on microglia promotes cell uptake of Alzheimer disease-associated amyloid β peptide. J Biol Chem 2006, 281:3651–3659

13. Liu Y, Walter S, Stagi M, Cherny D, Letiembre M, Schulz-Schaeffer W, Heine H, Penke B, Neumann H, Fassbender K: LPS receptor (CD14): a receptor for phagocytosis of Alzheimer's amyloid peptide. Brain 2005, 128:1778–1789

14. Xie Z, Wei M, Morgan TE, Fabrizio P, Han D, Finch CE, Longo VD: Peroxynitrite mediates neurotoxicity of amyloid β-peptide1-42- and lipopolysaccharide-activated microglia. J Neurosci 2002, 22:3484–3492

15. Takeuchi H, Jin S, Wang J, Zhang G, Kawanokuchi J, Kuno R, Sonobe Y, Mizuno T, Suzumura A: Tumor necrosis factor-α induces neurotoxicity via glutamate release from hemichannels of activated microglia in an autocrine manner. J Biol Chem 2006, 281:21362–21368

16. Suzumura A, Mezitis SG, Gonatas NK, Silberberg DH: MHC antigen expression on bulk isolated macrophage-microglia from newborn mouse brain: induction of Ia antigen expression by γ-interferon. J Neuroimmunol 1987, 15:263–278

17. Naiki H, Nakakuki K: First-order kinetic model of Alzheimer's β-amyloid fibril extension in vitro. Lab Invest 1996, 74:374–383

18. Dahlgren KN, Manelli AM, Stine WB Jr, Baker LK, Krafft GA, LaDu MJ: Oligomeric and fibrillar species of amyloid-β peptides differentially affect neuronal viability. J Biol Chem 2002, 277:32046–32053

19. Pollock JS, Forstermann U, Mitchell JA, Warne TD, Schmidt HHHW, Nakane M, Murad F: Purification and characterization of particulate endothelium-derived relaxing factor synthase from cultured and native bovine aortic endothelial cells. Proc Natl Acad Sci USA 1991, 88:10480–10484

20. Takeuchi H, Mizuno T, Zhang G, Wang J, Kawanokuchi J, Kuno R, Suzumura A: Neuritic beading induced by activated microglia is an early feature of neuronal dysfunction toward neuronal death by inhibition of mitochondrial respiration and axonal transport. J Biol Chem 2005, 280:10444–10454

21. Lesné S, Koh MT, Kotilinek L, Kayed R, Glabe CG, Yang A, Gallagher M, Ashe KH: A specific amyloid-β protein assembly in the brain impairs memory. Nature 2006, 440:352–357

22. Maurice T, Lockhart BP, Privat A: Amnesia induced in mice by centrally administered β-amyloid peptides involves cholinergic dysfunction. Brain Res 1996, 706:181–193

23. Alkam T, Nitta A, Mizoguchi H, Itoh A, Nabeshima T: A natural scavenger of peroxynitrites, rosmarinic acid, protects against impairment of memory induced by Aβ (25-35). Behav Brain Res 2007, 180:139–145

24. Kamei H, Nagai T, Nakano H, Togan Y, Takayanagi M, Takahashi K, Kobayashi K, Yoshida S, Maeda K, Takuma K, Nabeshima T, Yamada K: Repeated methamphetamine treatment impairs recognition memory through a failure of novelty-induced ERK1/2 activation in the prefrontal cortex of mice. Biol Psychiatry 2006, 59:75–84

25. Mizoguchi H, Takuma K, Fukakusa A, Ito Y, Nakatani A, Ibi D, Kim HC, Yamada K: Improvement by minocycline of methamphetamine-induced impairment of recognition memory in mice. Psychopharmacology 2008, 196:233–241

26. Mouri A, Noda Y, Hara H, Mizoguchi H, Tabira T, Nabeshima T: Oral vaccination with a viral vector containing Aβ cDNA attenuates agerelated Aβ accumulation and memory deficits without causing inflammation in a mouse Alzheimer model. FASEB J 2007, 21:2135–2148

27. Franklin KBJ, Paxinos G: The mouse brain: in stereotaxic coordinates. San Diego, Academic 1997, pp. 69–89

28. Scholtzova H, Kascsak RJ, Bates KA, Boutajangout A, Kerr DJ, Meeker HC, Mehta PD, Spinner DS, Wisniewski T: Induction of Toll-like receptor 9 signaling as a method for ameliorating Alzheimer's disease-related pathology. J Neurosci 2009, 29:1846–1854

29. Lee TS, Chau LY: Heme oxygenase-1 mediates the anti-inflammatory effect of interleukin-10 in mice. Nat Med 2002, 8:240–246

30. Krug A, Rothenfusser S, Hornung V, Jahrsdorfer B, Blackwell S, Ballas ZK, Endres S, Krieg AM, Hartmann G: Identification of CpG oligonucleotide sequences with high induction of IFN-α/β in plasmacytoid dendritic cells. Eur J Immunol 2001, 31:2154–2163

31. Selkoe DJ: Alzheimer's disease is a synaptic failure. Science 2002, 298:789–791

32. Demuro A, Mina E, Kayed R, Milton SC, Parker I, Glabe CG: Calcium dysregulation and membrane disruption as a ubiquitous neurotoxic mechanism of soluble amyloid oligomers. J Biol Chem 2005, 280:17294–17300

33. Shankar GM, Bloodgood BL, Townsend M, Walsh DM, Selkoe DJ, Sabatini BL: Natural oligomers of the Alzheimer amyloid-β protein induce reversible synapse loss by modulating an NMDA-type glutamate receptor-dependent signaling pathway. J Neurosci 2007, 27:2866–2875

34. Knobloch M, Farinelli M, Konietzko U, Nitsch RM, Mansuy IM: Aβ oligomer-mediated long-term potentiation impairment involves protein phosphatase 1-dependent mechanisms. J Neurosci 2007, 27:7648–7653

35. Townsend M, Mehta T, Selkoe DJ: Soluble Aβ inhibits specific signal transduction cascades common to the insulin receptor pathway. J Biol Chem 2007, 282:33305–33312

36. Manelli AM, Bulfinch LC, Sullivan PM, LaDu MJ: Aβ42 neurotoxicity in primary co-cultures: effect of apoE isoform and Abeta conformation. Neurobiol Aging 2007, 28:1139–1147

37. Lue LF, Walker DG, Rogers J: Modeling microglial activation in Alzheimer's disease with human postmortem microglial cultures. Neurobiol Aging 2001, 22945–956

38. Combs CK, Karlo JC, Kao SC, Landreth GE: β-Amyloid stimulation of microglia and monocytes results in TNF α-dependent expression of inducible nitric oxide synthase and neuronal apoptosis. J Neurosci 2001, 21:1179–1188

39. Tahara K, Kim HD, Jin JJ, Maxwell JA, Li L, Fukuchi K: Role of Toll-like receptor signalling in Aβ uptake and clearance. Brain 2006, 129:3006–3019

40. Maines MD: The heme oxygenase system: a regulator of second messenger gases. Annu Rev Pharmacol Toxicol 1997, 37:517–554

41. Atamna H, Frey WH II: A role for heme in Alzheimer's disease: heme binds amyloid β and has altered metabolism. Proc Natl Acad Sci USA 2004, 101:11153–11158

42. Takahashi M, Doré S, Ferris CD, Tomita T, Sawa A, Wolosker H, Borchelt DR, Iwatsubo T, Kim SH, Thinakaran G, Sisodia SS, Snyder SH: Amyloid precursor proteins inhibit heme oxygenase activity and augment neurotoxicity in Alzheimer's disease. Neuron 2000, 28:461–473

43. Lee HY, Kim MK, Park KS, Bae YH, Yun J, Park JI, Kwak JY, Bae YS: Serum amyloid A stimulates matrix-metalloproteinase-9 up-regulation via formyl peptide receptor like-1-mediated signaling in human monocytic cells. Biochem Biophys Res Commun 2005, 330:989–998

44. Dalpke AH, Schäfer MK, Frey M, Zimmermann S, Tebbe J, Weihe E, Heeg K: Immunostimulatory CpG-DNA activates murine microglia. J Immunol 2002, 168:4854–4863

45. Iliev AI, Stringaris AK, Nau R, Neumann H: Neuronal injury mediated via stimulation of microglial Toll-like receptor-9 (TLR9). FASEB J 2004, 18:412–414

46. Krieg AM: Therapeutic potential of Toll-like receptor 9 activation. Nat Rev Drug Discov 2006, 5:471–484

47. Meyer-Luehmann M, Spires-Jones TL, Prada C, Garcia-Alloza M: de Calignon A. Rozkalne A, Koenigsknecht-Talboo J, Holtzman DM, Bacskai BJ, Hyman BT: Rapid appearance and local toxicity of amyloid-β plaques in a mouse model of Alzheimer's disease. Nature 2008, 451:720–724

48. Mandrekar S, Jiang Q, Lee CY, Koenigsknecht-Talboo J, Holtzman DM, Landreth GE: Microglia mediate the clearance of soluble Aβ through fluid phase macropinocytosis. J Neurosci 2009, 29:4252–4262

49. Wu HJ, Sawaya H, Binstadt B, Brickelmaier M, Blasius A, Gorelik L, Mahmood U, Weissleder R, Carulli J, Benoist C, Mathis D: Inflammatory arthritis can be reined in by CpG-induced DC-NK cell cross-talk. J Exp Med 2007, 204:1911–1922

50. Stevens SL, Ciesielski TM, Marsh BJ, Yang T, Homen DS, Boule JL, Lessov NS, Simon RP, Stenzel-Poore MP: Toll-like receptor 9: a new target of ischemic preconditioning in the brain. J Cereb Blood Flow Metab 2008, 28:1040–1047

# Mechanism Underlying Apolipoprotein E (ApoE) Isoform-dependent Lipid Efflux From Neural Cells in Culture

Hirohisa Minagawa,[1] Jiang-Sheng Gong,[1] Cha-Gyun Jung,[1] Atsushi Watanabe,[2] Sissel Lund-Katz,[3] Michael C. Phillips,[3] Hiroyuki Saito,[4] and Makoto Michikawa[1]★

[1]Department of Alzheimer's Disease Research, National Institute for Longevity Sciences,
National Center for Geriatrics and Gerontology, Aichi, Japan
[2]Department of Vascular Dementia, National Institute for Longevity Sciences,
National Center for Geriatrics and Gerontology, Aichi, Japan
[3]Lipid Research Group, Children's Hospital of Philadelphia, University of Pennsylvania School
of Medicine, Philadelphia, Pennsylvania
[4]Department of Biophysical Chemistry, Kobe Pharmaceutical University, Kobe, Japan

We determined the molecular mechanisms underlying apolipoprotein E (ApoE)-isoform-dependent lipid efflux from neurons and ApoE-deficient astrocytes in culture. The ability of ApoE3 to induce lipid efflux was 2.5- to 3.9-fold greater than ApoE4. To explore the contributions of the amino- and carboxyl-terminal tertiary structure domains of ApoE to cellular lipid efflux, each domain was studied separately. The amino-terminal fragment of ApoE3 (22-kDa-ApoE3) induced lipid efflux greater than 22-kDa-ApoE4, whereas the common carboxyl-terminal fragment of ApoE induced very low levels of lipid efflux. Addition of segments of the carboxyl-terminal domain to 22-kDa-ApoE3 additively induced lipid efflux in a length-dependent manner; in contrast, this effect did not occur with ApoE4. This observation, coupled with the fact that introduction of the E255A mutation (which disrupts domain–domain interaction) into ApoE4 increases lipid efflux, indicates that interaction between the amino- and carboxyl-terminal domains in ApoE4 reduces the ability of this isoform to mediate lipid efflux from neural cells. Dimeric 22-kDa or intact ApoE3 induced higher lipid efflux than monomeric 22-kDa or intact ApoE3, respectively, indicating that dimerization of ApoE3 enhances the ability to release lipids. The adenosine triphosphate–binding cassette protein A1 (ABCA1) is involved in ApoE-induced lipid efflux. In conclusion, there are two major factors, intramolecular domain interaction and intermolecular dimerization, that cause ApoE-isoform-dependent lipid efflux from neural cells in culture. © 2009 Wiley-Liss, Inc.

Key words: Alzheimer's disease; apolipoprotein E; high-density lipoprotein (HDL); neurons; astrocyte

The lipoprotein found in the central nervous system (CNS) is the high-density lipoprotein (HDL), and apolipoprotein E (ApoE) is one of the major apolipoproteins regulating lipid transport in CNS (Roheim et al.,

1979; Pitas et al., 1987b; Weisgraber et al., 1994). Astrocytes and microglia synthesize and secrete ApoE (Boyles et al., 1985; Nakai et al., 1996), which interacts with adenosine triphosphate (ATP)-binding cassette protein A1 (ABCA1) (Krimbou et al., 2004) to remove cholesterol from cells and generate HDL particles in the cerebrospinal fluid and cultured media (Pitas et al., 1987a; Borghini et al., 1995; LaDu et al., 1998).

ApoE-inducible lipid efflux is ApoE-isoform dependent (Michikawa et al., 2000; Gong et al., 2002; Xu et al., 2004), and ApoE3 generates a similar number of HDL particles to but with a smaller number of ApoE molecules than ApoE4 (Gong et al., 2002). HDL synthesis mediated by ApoE contributes to cholesterol release from the cell membrane. On the other hand, HDL associated with ApoE is taken up by cells via ApoE receptors and the cholesterol in HDL is used for maintaining cholesterol homeostasis in CNS neurons. Thus, this isoform-specific action of ApoE to remove cholesterol and

generate HDL may be the cause of altered cholesterol metabolism in an Alzheimer's disease (AD) brain (Demeester et al., 2000; Molander-Melin et al., 2005) and may explain how ApoE4 serves as a strong risk factor for AD development (Corder et al., 1993; Strittmatter et al., 1993). However, the molecular mechanism underlying ApoE-isoform-dependent HDL generation remains to be elucidated.

The ApoE molecule has two distinct domains, namely, the 22-kDa amino-terminal (residues 1–191) and 10-kDa carboxyl-terminal domains (residue 218–299), that unfold independently of each other (Wetterau et al., 1988; Morrow et al., 2000). It has been demonstrated that ApoE4 amino- and carboxyl-domain interaction is responsible for the ApoE-isoform dependent association with lipid particles (Weisgraber, 1990; Dong and Weisgraber, 1996; Saito et al., 2003). The domain interaction in ApoE4 under physiological conditions has also been confirmed at the cellular level (Xu et al., 2004) and in vivo (Raffai et al., 2001; Ramaswamy et al., 2005), suggesting that the presence or absence of the domain interaction can explain ApoE-isoform dependent lipid efflux. In addition, there are ApoE-isoform dependent differences in the structure and stability of the 22-kDa amino-terminal fragment (22-kDa-ApoE), which affect their binding affinities to lipids (Morrow et al., 2000, 2002; Segall et al., 2002; Hatters et al., 2005), suggesting that the 22-kDa-ApoE that lacks the domain interaction may also explain an isoform-dependent lipid efflux.

In this study, we investigated the molecular mechanisms, by which intact ApoE3 has a greater ability to induce cholesterol efflux than intact-ApoE4 by using cultured rat neurons and astrocytes prepared from ApoE knockout mouse brain to exclude the effect of endogenously generated and secreted ApoE. We found that the intramolecular amino- and carboxyl-terminal domain interaction is partially responsible for this ApoE-isoform dependency. To our surprise, 22-kDa-ApoE3 has a greater ability to induce cholesterol efflux than 22-kDa-ApoE4. This is because 22-kDa-ApoE3 forms dimers, whereas 22-kDa-ApoE4 does not. These findings suggest that cholesterol efflux induced by ApoE is regulated by two major factors: the presence or absence of intermolecular dimer formation and the intramolecular domain interaction.

## EXPERIMENTAL PROCEDURES

### Cell Culture

All experiments were performed in compliance with existing laws and institutional guidelines. Neuron-rich cultures were prepared from rat cerebral cortices as previously described (Michikawa et al., 2001). Cerebral cortices from rat brains were dissected, freed of meninges, and diced into small fragments. Cortical fragments were incubated in 2.5% trypsin and 2 mg/ml DNase I in phosphate-buffered saline (PBS) (8.1 mM $Na_2HPO_4$, 1.5 mM $KH_2PO_4$, 137 mM NaCl, and 2.7 mM KCl; pH 7.4) at 37°C for 15 min. The fragments were then dissociated into single cells by pipetting. The dissociated

cells were suspended in a feeding medium and plated onto poly-D-lysine-coated 12-well plates at a cell density of 1 × $10^6$/ml in Dulbecco modified Eagle's medium nutrient mixture (DMEM/F-12; 50:50%) containing $N_2$ supplements plus 7.5% bovine albumin fraction V.

Highly astrocyte-rich cultures were prepared according to a previously described method (Michikawa et al., 2001). In brief, brains of postnatal day 2 ApoE knockout mice were removed under anesthesia. The cerebral cortices from the mouse brains were dissected, freed of meninges, and diced into small fragments. Cortical fragments were incubated in 0.25% trypsin and 2 mg/ml DNase I in PBS (8.1 mM $Na_2HPO_4$, 1.5 mM $KH_2PO_4$, 137 mM NaCl and 2.7 mM KCl; pH 7.4) at 37°C for 15 min. The fragments were then dissociated into single cells by pipetting. The dissociated cells were seeded in 75-cm² dishes at a cell density of 1 × $10^7$ in DMEM nutrient mixture containing 10% FBS and 1% penicillin/streptomycin solution (Invitrogen Corporation, Carlsbad, CA). After 10 days of incubation in vitro, astrocytes in the monolayer were trypsinized (0.1%) and reseeded onto twelve-well dishes. The astrocyte-rich cultures were maintained in DMEM containing 10% FBS until use.

### ApoE Preparation

The full-length human ApoE3 and ApoE4 and their 22- and 10-kDa fragments were expressed and purified as described (Saito et al., 2001). The cDNA for full-length human ApoE3 and ApoE4, the 22-kDa fragments, or the 10-kDa fragment were ligated into a thioredoxin fusion expression vector pET32a and transformed into the *Escherichia coli* strain BL21 star (DE3). The transformed *E. coli* were cultured in LB medium at 37°C, and thioredoxin-ApoE expression was induced with iso-propyl-β-D-galactopyranoside for 3 hr. After the bacterial pellet was sonicated and the lysate was centrifuged to remove debris, the fusion protein was cleaved with thrombin to remove thioredoxin from full-length ApoE3, ApoE4 or the 22- or 10-kDa fragment. For the full-length ApoE3 and ApoE4, the fusion protein was complexed with DMPC before it was cleaved with thrombin to protect the protease susceptible internal hinge region. After inactivation of the thrombin with β-mercaptoethanol, the mixture was lyophilized and delipidated, and the ApoE pellet was dissolved in 6 M guanidine–HCl, pH 7.4, containing 1% β-mercaptoethanol. The ApoE was isolated by gel filtration chromatography on a Sephacryl S-300 column. For further purification (>95%), the proteins were subjected to gel filtration with a Superdex 75 column or anion exchange chromatography with a HiTrap Q column

When we used ApoE and ApoE fragments, the recombinant ApoEs were dissolved in 5 M guanidine–HCl. The resulting solutions were dialyzed against PBS at 4°C for 16 hr. Each ApoE level was determined with a BCA protein assay kit (Pierce, Rockford, IL).

### Determination of Levels of Cholesterol and Phosphatidylcholine (PC) Released From Neurons and Astrocytes Labeled With [¹⁴C]acetate

Astrocytes plated in twelve-well dishes were cultured in DMEM containing 10% FBS and 1% penicillin/streptomycin

solution for 72 hr. The cultures were then treated with 37 kBq/ml [$^{14}$C]acetate (Moravek Biochemicals Inc., Brea, CA) for 48 hr. The astrocytes were washed in DMEM two times and treated with 0.3 µM ApoE in DMEM for 24 hr. To analyze dose-dependent effects, the astrocytes were treated with 0.03 µM, 0.1 µM, 0.3 µM and 1.0 µM ApoE; to analyze time-dependent effects, the astrocytes were treated and maintained for 8, 24 and 48 hr. The culture medium was quickly removed and the astrocytes were dried at room temperature. 1.0 ml of the conditioned culture medium was extracted with 4.0 ml of hexane/isopropyl alcohol (3:2 v/v). For the extraction of intracellular lipids, dried astrocytes were incubated in hexane/isopropyl alcohol (3:2 v/v) for 1 hr at room temperature. The solvent from each plate was removed and dried under N$_2$ gas. The organic phase was redissolved in 200 µl of hexane/isopropyl alcohol (3:2 v/v), and 10 µl of each sample was spotted on activated-silica-gel high- performance thin layer chromatography plates (Merck); the lipids were separated by sequential one-dimensional chromatography by using chloroform/methanol/acetic acid/water (25:15:4:2, v/v), followed by another run in hexane/diethyl ether/acetic acid (80:30:1). [$^{14}$C]Cholesterol and [$^{14}$C]PC were used as standards. The chromatography plates were exposed to radiosensitive films, and each lipid was visualized and quantified with BAS2500 (Fuji Film, Tokyo, Japan). The levels of [$^{14}$C]cholesterol and [$^{14}$C]PC efflux were calculated by the following formula: % efflux = media × 100/(media + cell).

### Dimerization of 22-kDa-ApoE3

The pure 22-kD-ApoE3 was obtained by reduction with 10 mM dithiothreitol (DTT) in 5 M guanidine–HCl buffer. The dimer was formed by incubation of the monomer in oxygenated 5 M guanidine–HCl at 10 mg/ml for 2 weeks at 4°C. Residual monomer was removed by passage of the protein solution through a thiopropyl Sepharose 6B column (GE Healthcare, Piscataway, NJ) according to the manufacturer's instructions.

### Dimerization of Intact ApoE3

The ApoE3 (1 mg/ml in 6 M urea, and 10 mM Tris-HCl) used was a mixture of monomeric and dimeric ApoEs. The mixture was reduced to generate monomeric ApoE3 by adding 10 mM DTT, incubated at 4°C for 16 hr, dialyzed against 6 M urea in 10 mM Tris-HCl solution, and oxidized by stirring at 4°C for 3 days. Then it was loaded onto a 2-ml-bed-volume prepacked 6% cross-linked beaded agarose gel column with a SulfoLink kit (Pierce, Rockford, IL) and equilibrated with PBS. Dimeric ApoE3 was eluted with PBS.

### Western Blot Analysis of Dimeric 22-kDa-ApoE3 by Nonreducing Gel Electrophoresis

To determine the ratio of dimeric 22-kDa-ApoE3 in the solution, Western blot analysis was performed under nonreducing conditions. Dimeric 22-kDa-ApoE3 was mixed with the same volume of a 2× nonreducing Laemmli buffer consisting of 100 mM Tris-HCl (pH 7.4), 10% glycerol, 4% SDS, and 0.01% bromophenol blue, and analyzed by 4–12% Tris/Tricine sodium dodecyl sulfate–polyacrylamide gel electropho-

resis (SDS-PAGE) (Daiichi Pure Chemicals Co., Tokyo, Japan). The separated proteins were transferred onto Immobilon membranes with a semidry electrophoretic transfer apparatus (Nihon Eido, Tokyo, Japan) with a transfer buffer (0.1 M Tris-HCl (pH 7.4), 0.192 M glycine, and 20% methanol). The blots were probed for 16 hr at 4°C with a goat anti-ApoE polyclonal antibody, AB947 (1:2,000; Chemicon, Temecula, CA). Band detection was carried out with an ECL kit (GE Healthcare UK Ltd., England).

### Purification and Carboxamidomethylation of Recombinant Intact ApoE3

ApoE3 was dissolved in 5 M guanidine–HCl, 10 mM EDTA, 200 mM Tris-HCl (pH8.5), and half of each protein solution was reduced with 10 mM DTT at room temperature for 2 hr and alkylated with 40 mM iodoacetamide in the dark at room temperature for 30 min, as described previously (Franceschini et al., 1990). All the proteins were then purified on an Aquapore RP300 column (2.1 × 30 mm; Applied Biosystems; Foster City, CA) by reverse-phase high–performance liquid chromatography (HPLC; model 1100 Series; Agilent Technology, Waldbronn, Germany) with a linear gradient of 36–52% acetonitrile in 0.1% trifluoroacetic acid for 16 min and a linear gradient of 52–76% acetonitrile in 0.1% trifluoroacetic acid for 1 min at a flow rate of 0.2 ml/min. The HPLC-purified ApoE3 was lyophilized and kept at −30°C until use.

### Effect of 22-hydroxycholesterol and Glyburide on 22-kDa-ApoEs-induced Lipid Efflux

Neuron cultures were prepared, maintained, and labeled with [$^{14}$C]acetate, and exposed to 22-kDa-ApoE3 dimer or 22-kDa-ApoE3 monomer at a concentration of 0.3 µM in the presence of 22-hydroxycholesterol (10 µM) or glyburide (500 µM) for 24 hr. The lipids released into the media and the lipids retained in the cells were then determined. The expression level of ABCA1 in the cultures for each treatment was determined by Western blot analysis with anti-ABCA1 antibody (Santa Cruz, Santa Cruz, CA) used as a primary antibody.

### RNA Interference

To knock down the endogenous ABCA1, primary cultured neurons and astrocytes were transiently transfected with 50 nM of the synthesized small interfering RNAs (siRNAs) targeting ABCA1 or with the Stealth siRNA negative control (Invitrogen) with Lipofectamine RNAiMAX (Invitrogen) according to the manufacturer's protocol. ABCA1 siRNA sequences is as follows: ABCA1-siRNA sense (5′-CA GGAUUUCCUGGUGGACAAUGAAA-3′) and antisense (5′-UUUCAUUGUCCACCAGGAAAUCCUG-3′).

### Statistical Analysis

StatView computer software (Windows) was used for statistical analysis. The statistical significance of differences between samples was evaluated by multiple pairwise comparisons among the sets of data by ANOVA and the Bonferroni t-test.

# RESULTS

Primary-cultured neurons and astrocytes were prepared and the levels of cholesterol and PC efflux were determined as described in Experimental Procedures. The levels of cholesterol and PC released from neurons in the medium treated with ApoE3 at 0.3 μM were significantly greater than those in the medium treated with ApoE4 (Fig. 1A). The level of cholesterol released by ApoE4 was 25% of that released by ApoE3. The reduced levels of cholesterol and PC efflux induced by ApoE4 increased significantly, although not to the level induced by ApoE3, when the neurons were incubated with the apoE4 (E255A) mutant (mt-ApoE4), which has altered amino- and carboxyl-terminal domain interaction because there is no electrostatic interaction between Arg61 and Glu255 (Dong and Weisgraber, 1996) (Fig. 1A). The partial recovery in the level of lipid efflux induced by mt-ApoE4 suggests that mechanisms other than the domain interaction are involved in ApoE-isoform-dependent lipid efflux from neurons in culture. Similar results were observed with cultured astrocytes. The levels of cholesterol and PC released from astrocytes in the medium treated with ApoE3 at 0.3 μM were significantly greater than those in the medium treated with ApoE4 (Fig. 1B). The levels of cholesterol and PC efflux induced by ApoE4 increased significantly, although not to the level induced by ApoE3, when the astrocytes were incubated with mt-ApoE4 (Fig. 1B).

We also examined the effect of the ApoE fragments on lipid efflux from cultured neurons and astrocytes to determine which part of the ApoE molecule is responsible for lipid efflux and ApoE isoform dependency. Interestingly, the 22-kDa fragment of ApoE (22-kDa-ApoE) induced cholesterol and PC efflux, which were ApoE-isoform-dependent (Fig. 1A,B). Unexpectedly, the carboxyl-terminal 10-kDa-ApoE and 12-kDa-ApoE, both of which contain the lipid binding site, have a very weak ability to release lipids (Fig. 1A,B).

Figure 2A shows the time-dependent cholesterol and PC efflux from neurons induced by 22-kDa-ApoE3 and 22-kDa-ApoE4 at 0.3 μM. The level of lipids released by 22-kDa-ApoE3 was significantly greater than that by 22-kDa-ApoE4 at time points of 24 and 48 hr (Fig. 2B). The level of cholesterol and PC efflux induced by 22-kDa-ApoE 24 hr after the treatment increased in an ApoE-concentration-dependent manner (Fig. 2B). The levels of cholesterol and PC efflux induced by 22-kDa-ApoE3 were greater than those released by 22-kDa-ApoE4 at 0.3 and 1.0 μM (Fig. 2B). Time- and ApoE-dose-dependent lipid efflux was also examined with ApoE-deficient astrocyte cultures, and the similar results were observed (Fig. 2C,D).

The results in Figures 1 and 2 indicate that the amino-terminal domain, the 22-kDa fragment, induces lipid efflux in an ApoE-isoform dependent manner, whereas the carboxyl-terminal domain, the 10-kDa fragment, has a very weak ability to induce lipid efflux from cultured astrocytes. These results raise the question of how the amino-terminal and carboxyl-terminal domains
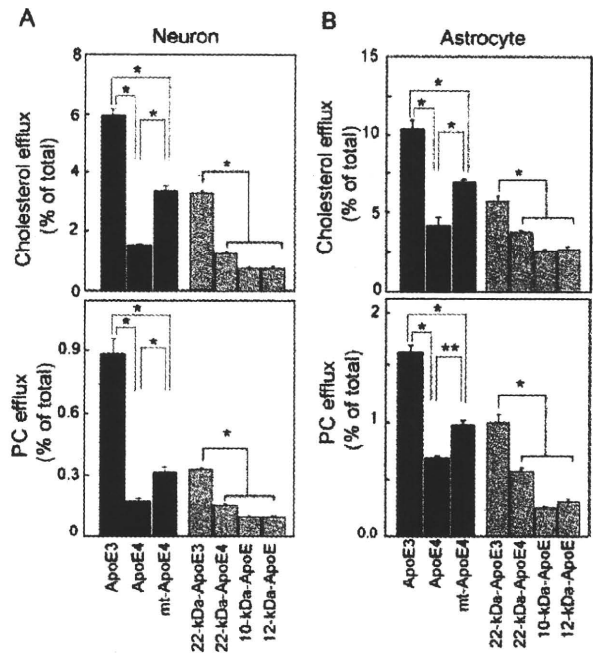
Fig. 1. Cholesterol and PC efflux from cultured neurons and astrocytes induced by ApoEs. Neurons and astrocytes were prepared as described in Experimental Procedures. The neurons (A) and astrocytes (B) were cultured for 72 hr, labeled with [$^{14}$C]acetate for 48 hr, and exposed to intact, lipid-free, ApoE3(residues 1–299), ApoE4, mt-ApoE4(E255A), 22-kDa-ApoE3 (residues 1–191), 22-kDa-ApoE4, 10-kDa-ApoE (residues 218–299), and 12-kDa-ApoE (residues 192–299) fragments at 0.3 μM for 24 hr. The lipids released into the media and the lipids retained in the cells were extracted and analyzed as described in Experimental Procedures. The percentages of released cholesterol and PC levels over the total levels were calculated. Data are means ± SE of four samples. $*P < 0.0001$ and $**P < 0.0005$. Three independent experiments showed similar results. The basal value of cholesterol and PC efflux in the absence of ApoEs are $1.0 ± 0.1$ (%) and $0.4 ± 0.1$ (%), respectively.

contribute to lipid efflux induced by intact ApoE in an ApoE-isoform-dependent manner. To answer this question, we examined whether the carboxyl-terminal domain of ApoE modifies lipid efflux caused by 22-kDa-ApoE. The ApoEs used were 22-kDa-ApoE (amino acids, 1–191) and 22-kDa-ApoE with carboxyl-terminal fragment of various lengths, that is, ApoEs harboring amino acids 1–250, 1–260, 1–272, and 1–299 (intact ApoE). As shown in Figure 3A, cholesterol and PC efflux induced by ApoE3 species from cultured neurons depended on the carboxyl-terminal fragment length; that is, ApoE3 variants with a longer carboxyl-terminal region induced progressively more lipid efflux. However, such is not the case for ApoE4. The addition of a carboxyl-terminal region ending at amino acid 250 increased the level of lipid efflux significantly more than 22-kDa-ApoE4; however, 22-kDa-ApoE4 with a car-